Fall 1-1-2016

Utilization of Fluorescent Chemosensors to Quantify Pb2+ in Aqueous Media

Aria Parangi

UTILIZATION OF FLUORESCENT CHEMOSENSORS TO QUANTIFY PB^{2+} IN AQUEOUS MEDIA

A Graduate Thesis

Submitted to the Bayer School of Natural and Environmental Sciences

Duquesne University

In partial fulfillment of the requirement for

the degree of Master of Science

By

Aria Parangi

December 2016

UTILIZATION OF FLUORESCENT CHEMOSENSORS TO QUANTIFY PB^{2+} IN AQUEOUS MEDIA

By

Aria Parangi

Approved October 24th, 2016

_____	_____
Dr. Partha Basu Professor of Chemistry & Biochemistry	Dr. Theodore A. Corcovilos Assistant Professor of Physics
_____	_____
Dr. John F. Stolz Director, Center for Environmental Research and Education Professor, Environmental Microbiology	Dr. Phillip P. Reeder Dean and Professor, Bayer School of Natural and Environmental Sciences

ABSTRACT

UTILIZATION OF FLUORESCENT CHEMOSENSORS TO QUANTIFY PB^{2+} IN AQUEOUS MEDIA

By

Aria Parangi

December 2016

Graduate thesis supervised by Dr. Partha Basu

Currently the detection of environmental lead samples requires time and material intensive methods. Recently, through the development of small fluorescent lead sensors, it may be possible to detect lead in the environment quickly and efficiently. A specific fluorescent chemosensor, Leadglow (LG), has shown promise in detecting low levels of lead in a rapid manner with little sample preparation or training. Leadglow and a naphthalene derivative were successfully synthesized and purified. The lead binding properties of Leadglow and the naphthalene derivative were studied and optimized. The use of Leadglow on several portable devices was also studied.

DEDICATION

This thesis is dedicated to my family and in particular my parents. They have stood by me every step of the way with unconditional love and support.

ACKNOWLEDGEMENT

First and foremost, I would like to thank my advisor, Dr. Partha Basu, who has mentored and guided me every step of my project. Dr. Basu believed in me and my abilities, even when I did not believe in myself. He pushed me to become not only a better scientist, but also a better person. Without his help I would not have accomplished nearly as much as I have.

Secondly I would like to thank Dr. Corcovilos and the Corcovilos research group, especially Gage Tiber who built and put together the circuitry and electronics for the device. Dr. Corcovilos helped make the idea of a portable device into a fully functioning prototype. If it wasn't for his expertise and dedication the device would still be nothing more than an idea.

In addition, I would like to thank Dr. John Stolz and Institute of Professional Environmental Practice (IPEP) who provided funding and guidance throughout the entire process, and who made this project possible. I would also like to acknowledge Dr. Michael Van Stipdonk for providing access to an accurate balance and Dr. Skip Kingston, who allowed me to use his ultrapure water to complete my project.

I would also like to thank the Basu research group, who was there every step of the way throughout the project. Whether discussing complex scientific principles or how life is for a grad student, they were always happy to help, even if it meant taking time out of their own project to do so.

Finally, I would like to thank Antoinette Peterson, who without her help, none of this would be possible. Ann passed down her knowledge and expertise on organic synthesis, data analysis and use of instrumentation, to name a few, in a methodical and efficient manner.

Without her guidance, I would not have been able to achieve my goals that I set out to accomplish.

TABLE OF CONTENTS

Appendix

LIST OF FIGURES

Chapter 1: Introduction

1.1 Introduction

The research project conducted consisted of two distinct goals with a few secondary subprojects within each goal. The first goal was to develop a protocol and optimize the procedure for the binding of LG to Pb^{2+}. The second goal was to test the binding of LG to Pb^{2+} on a portable fluorometer developed internally within Duquesne University. In the following document we describe the importance of these goals as well as the methods used to achieve these goals. The first section consists of a background of the health impacts of Pb^{2+}, current methods of detection as well as the use and development of fluorescent chemosensors. The second section consists of the materials and methods used to synthesize the LG compound and its naphthalene derivative as well as various spectroscopic methods used to confirm their synthesis. The third section consists of the development of a portable fluorometer to detect Pb^{2+} using the LG compound. The fourth section consists of the optimization of the binding of LG to Pb^{2+} by adjusting a number of environmental variables. The final section consists of testing water samples, taken from a local community, for Pb^{2+} using both a benchtop fluorometer and the portable fluorometer.

1.2 Impact of lead on human health

Lead is a heavy metal with no known biological function in the human body. As an environmental pollutant, lead can be dispersed between various media in nature and bioaccumulate in organisms.[2] The major routes of exposure to lead are through inhalation of dust particles, drinking of lead-contaminated water and ingestion of lead paint chips.[1,2] According to the World Health Organization (WHO), in adults more than 95% of total lead in the body is found in the bones, while in children only 73% is located in bone, the rest resides in red blood cells and tissue.[3] Recent studies by the Centers for Disease Control (CDC) indicate correlations between low levels of lead blood concentrations, <10 μg/dL, and a decrease in children IQ levels as well as behavioral issues such as ADHD and ADD.[5] Previous to 2012, the CDC's threshold for Blood Lead Levels (BLLs) of concern in children between 1 and 5 years old was 10 μg/dL, which corresponded to the 97.5th percentile of BLLs in that age range.[4,5,6] This threshold level was revised in 2012 to 5μg/dL based on data from the 2007-2008 and 2009-2010 National Health and Nutrition Examination Survey (NHANES).[4]

According to the EPA and CDC, the population most at risk includes children and pregnant women. Children are particularly susceptible due to their behavior and physiology.[8] For example, children are more likely to put non-food items containing lead into their mouth as well have a higher absorption rate of lead into their bodies via

the gastrointestinal tract, as compared to adults.[8] In addition, lead has been found to substitute for calcium in the human body and consequently interferes with mitochondrial respiration and proper neurological tissue function.[9]

Evens et. al published a study in Environmental Health in 2015 which analyzed the impact of low levels of lead on school children's performance in the Chicago public school system.[11] The study utilized data on blood lead levels from the Chicago Blood Lead Surveillance Program and the Chicago Birth Registry.[11] Using a sample size of 58,650 students and, the researchers concluded that a 5μg/dL increase in BLLs lead to a 32% increase in the risk of failure on the Illinois Standard Achievement Test (ISAT).[11] This statistic can be seen in Figure 1.

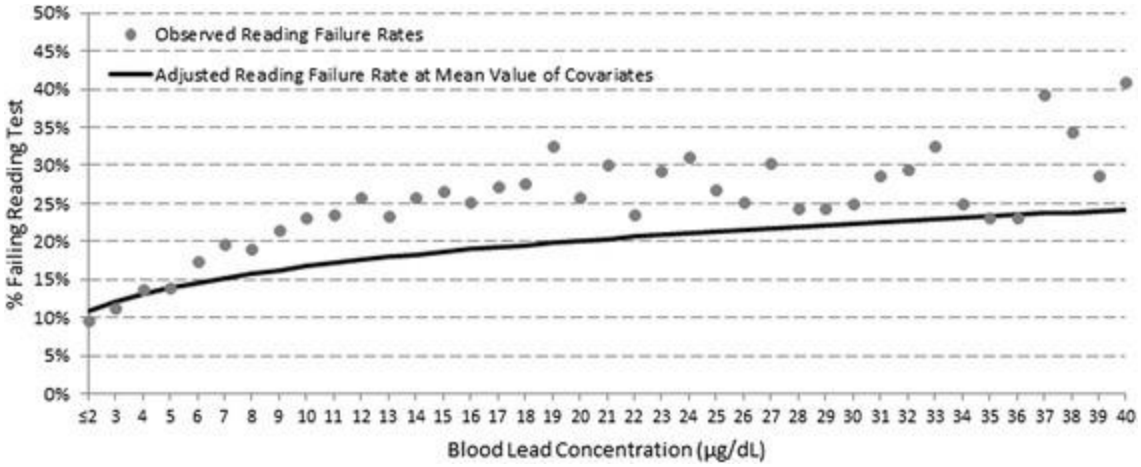

Figure 1: Higher reading failure rates on the ISAT with increasing Blood Lead Concentration among 58,650 school children in the Chicago public school system. Study reported in 2015 (open source).[11]

Despite the known environmental and human health impacts of lead, the US EPA has been slow to enact substantial regulations to curb its release into the environment as was evidenced by several high-profile incidents involving lead in water.

1.3 Lead regulations in the United States

Air

As part of Title I of the Clean Air Act (CAA), the EPA is required to set National Ambient Air Quality Standards (NAAQS) for criteria pollutants which are deemed to be harmful to human and environmental health. Lead is one of six criteria pollutants and has both primary standards, designated to protect public health, and secondary standards, designated to protect public welfare and environmental health. The current NAAQS for lead, 0.15μg/m^3 ,was revised in 2008 from the initial level of 1.5μg/m^3 set in 1978.[12]

Lead-based paint

On September 2nd, 1977 the United States Consumer Product Safety Commission (CPSC) issued a final ban on the use of lead-based paint in homes to reduce the risk of lead exposure to children.[10] In 1992, Congress passed the Residential Lead-Based Paint Hazard Reduction Act.[13] The act requires that people selling homes built before 1978

notify the buyer if lead-based paint is present in the house as well as provide an EPA-approved informational pamphlet which indicates the hazards of lead-based paint and how to identify for it.[13] If sellers do not follow these guidelines they can potentially face criminal charges.

Drinking water

On June 19th, 1986 the EPA amended the Safe Drinking Water Act (SDWA) to ban the use of lead pipes, solder or flux in public water systems.[14,15] Lead is currently regulated under the Lead and Copper Rule (LCR) of 1991 which sets the Maximum Contaminant Level Goal (MCLG) for lead at zero and changed the previous action level, the level at which a municipal water system must take action to reduce lead in the water supply, from 50ppb to 15ppb.[16,17] In addition, public water systems are required to monitor tap water samples which serve their municipality. [17] However, this water testing is often done at a cost to the municipalities and there can often be large fluctuations in lead concentrations which can skew the data. If 10 percent of them are above the EPA action limit, they must take steps to reduce the risk that lead in drinking water has on public health including implementing corrosion controls, educating the public on the hazards of lead and removing lead service pipes. Despite these regulatory changes, lead remains a serious environmental and human health issue due

to large quantity of old public water systems still in use that contain lead pipes and solder, such as in Flint, Michigan and Washington D.C.

The Flint and Washington D.C water crises demonstrated not only the need for proper management of water resources, but also a cheap, yet accurate, method to test lead in water in homes and businesses. In 2000, the D.C Water and Sewage Authority (WASA) decided to change their disinfectant method of drinking water from chlorine to chloramine as per the EPAs recommendation that chlorine and its byproducts could be linked to cancer. In 2003 WASA hired Dr. Marc Edwards of Virginia Tech to perform research into pipe corrosion in their water distribution systems and he found elevated levels of lead. Rather than accept Dr. Edwards' findings and add corrosion inhibitors to the water supply, the EPA and CDC deemed the water safe to drink and the lead levels were only temporary.

Similar to the D.C crisis, the Flint crisis occurred from cutting corners. In 2014, Flint switched its water source from Detroit to the more corrosive water from the Flint River to save money. After residents started complaining about the color and smell of their water, Dr. Edwards created 300 lead testing kits and sent them to 271 residences, 252 of whom (about an 84% return rate) mailed back the water samples to be tested using an ICP-MS.[18] According to Dr. Edwards, over 40% of the samples had lead levels over 5ppb and over 16% of the samples were above the EPA action limit of 15ppb.[18] Dr.

Edwards' results depended on residents collecting their own water samples and sending them back to Virginia Tech for analysis. This citizen sampling method demonstrates that normal residents are willing and able to test for lead in their own water, if they have the means to do so.

1.4 Current analytical techniques used to quantify lead

Current methods for detection of lead involve expensive and non-portable equipment, which require time-consuming sample preparation and have inadequacies on their limits of detection and use as shown in Table 1. The most prevalent methods include Inductively Coupled Plasma-Quadrupole-Mass Spectrometry (ICP-Q-MS), Flame Atomic Absorption Spectroscopy (FAAS), and Anodic Stripping Voltammetry (ASV).

Technique	Limit of Detection	Limitations	Cost Per Sample ($)[43,44,45]
ICP-Q-MS	0.0003 ppb[19]	Non-portable, extensive training, energy use and carrier gas costs	90
FAAS	0.01 ppb[23,24]	Non-portable, extensive sample preparation, large sample size	20-35
ASV	0.9-1.5 ppb[20]	Mercury electrode/electrode interference, limited number of detectable metal ions	0.30-4.40†

Table 1: ICP-Q-MS, FAAS and ASV comparison of detection limits and cost[19,20,23,43,44,45]

† Cost based on testing for arsenic[45]

ICP-Q-MS works by running a liquid or solid sample, through a nebulizer to transform the analyte into an aerosol. An inert carrier gas of either argon or helium (although helium is rarely used to due to its cost) carries the aerosol to the ionization torch.[22] Argon is subject to a strong magnetic field and a high energy spark, which forms a stream of highly ionized inductively coupled plasma between 6,000 K and 10,000 K, depending on the instrument.[19,22] The nebulized analyte is introduced into the plasma where it becomes ionized. Once ionized, the analyte goes through a quadrupole, consisting of four conductive rods, two of which have alternating current

(AC) running through the poles and the other two which have direct current (DC) running through the poles.[22] The quadrupole separates the ions based on the mass over charge (m/z) ratios. Only ions of a unique m/z ratio will hit the detector at a single time.[22] The signal from each ion is amplified via an electron multiplier and is correlated to the concentration of the ion present in the sample.[22]

ICP-Q-MS is a fast technique, requires little sample volume and is an accurate technique (1-3% for solution method).[19] However, it has a number of limitations. Samples with a high Total Dissolved Solids (TDS) content can impact the instrument's effectiveness by depositing solids onto the nebulizer and ionization chamber.[22] In addition, the sample is destroyed once it has been analyzed and cannot be recovered. Finally, this instrument requires extensive training to use and operate.

A less sensitive, but easier to use detection method is Flame Atomic Absorption Spectroscopy (FAAS). FAAS works through shining a specific wavelength of light on a sample and measuring how much of that light is absorbed and consequently correlating it to a concentration of analyte present in the sample. In order to ensure that only the element in question is measured, several steps need to take place. First, the analyte is introduced to a flame, usually an air-acetylene mix at 2,300 °C, which nebulizes the sample in order to remove any interferences from organic matrices.[24] Once nebulized, a hollow cathode lamp, with high intensity light excites the atoms in the sample, which

absorb light at specific wavelengths.[24] The light that the sample absorbs is passed through a monochromator which selects a particular wavelength of light.[24] This ensures that only the absorption of the analyte in question will be measured as other analytes will ideally not absorb light at that wavelength.[24] Once the light passes through the monochromator, it goes into a photomultiplier tube which amplifies the signal that the detector reads. At high concentrations the absorbance is correlated to the concentration of the analyte via the Beer-Lambert Law shown in Equation 1 where **A** is the absorbance, $\mathbf{I_0}$ is the incident light, **I** is the transmitted light, **ε** is the molar absorptivity in M^{-1} cm^{-1} , **L** is the path length in cm and **c** is the concentration in M.[25] For low concentrations, a linear approximation can be used to calculate the concentration of an analyte.

$$\mathbf{A = \log_{10} \frac{I_o}{I} = \varepsilon\, L\, c}$$

Equation 1

Unlike the electromagnetic technique used in ICP-Q-MS and optical technique used in FAAS, ASV utilizes the electrochemical properties of lead to determine lead concentration in a sample.

ASV can utilize two different types of electrodes when performing analyses: a Hanging Mercury Drop Electrode (HMDE) or a Thin-Film Mercury Electrode (TFME).

The HMDE method works by depositing a drop of elemental mercury (Hg) onto an inert electrode surface.[28] A negative potential is run across the electrode in order to reduce the lead ion in solution from Pb^{2+} to elemental lead, which deposits onto the mercury electrode surface and forms an amalgam with the mercury.[28] Then a positive potential is run across the electrode which oxidizes elemental lead and dissolves it back into solution, hence the stripping in ASV.[28] During the second step, the current is measured and correlates to the concentration of lead in solution. TFME uses a similar technique but with a number of mercury droplets.[28] This increases the surface area, allowing for a higher sensitivity, but cannot be regenerated. Both methods have limitations in that they require pre-treatment of samples with strong acids to destroy the organic matrix and they produce mercury waste, which is highly toxic and needs to be treated and handled properly. A more recent development has been to utilize small fluorescent chemosensors to qualitatively and quantitatively measure metal ion concentrations in a sample.

1.5 Fluorescent chemosensors

Fluorescence spectroscopy utilizes the phenomenon that when certain molecules absorb light or in the strict sense a photon, they excite electrons from the ground electronic state to an excited electronic state. When in the ground state, the electrons in the same molecular orbital will have opposite spins as they are degenerate, as per the

Pauli Exclusion Principle, and the total spin angular momentum will be zero, identified as the singlet state. Since spin angular momentum is conserved, the excited electron will retain the same spin as it had in the ground state. The electron then relaxes to the ground state and emits a photon in doing so, which is called fluorescence. This process takes between 10^{-8}s and 10^{-5}s to occur.[29] In some cases the excited electron undergoes intersystem crossing and will change spin. The spin angular momentum will change before the electron relaxes back down to the ground state configuration. Since this transition is forbidden, it is much less likely than fluorescence and will take longer to relax to ground state; on the order of 10^{-4}s to 10^{4} seconds.[29]

Fluorescent sensors offer several advantages when analyzing metal ions when compared to more traditional analytical techniques. They do not require extensive training, are sensitive and selective towards the ion being analyzed and are a cheap, quick method to analyze metal content in a sample.

Fluorescent chemosensors can analyze metal ion content through several photo-chemical processes. A common process involved in fluorescent chemosensors is Photoinduced Electron Transfer (PET). These fluorescent chemosensors often contain a nonbonding electron pair on an atom, such as nitrogen or sulfur, which can transfer those electrons to the chromophore present in the molecule.[32] This molecule containing the nonbonding electron pair is known as the donor.[32] The orbital of the non-binding

lone pair lies between the Highest Occupied Molecular Orbital (HOMO) and the Lowest Unoccupied Molecular Orbital (LUMO).[32] During PET, the initially excited electron from the LUMO will transfer to the lone pair orbital via a non-radiative process and the fluorescent signal will then be quenched or turned-off.[32] However, when bonding occurs with another atom or metal ion, also known as the acceptor in this system, the acceptor is able to coordinate to the lone pair, and reduction-oxidation chemistry occurs, lowering the energy of the binding orbital.[32,33] This will prevent PET from occurring in the molecule, resulting in a turn-on response. When metal ions act as the acceptor in this system, the phenomenon is referred to as Chelation Enhanced Fluorescence (CHEF). This process is common in quinoline-based chemosensors as shown in Figure 2 , however detection of metal ions is limited by small Stokes shifts and therefore overlap between the emission and absorption spectra, which can lead to difficulties in quantifying metal ion concentrations in a sample.[30,33] Cai-ling et. al have developed a Cu^{2+} chemosensor, N-(2-hydroxyl-naphthylmethyl)-N-(quinol-8-yl) amine, which exhibits a turn-on response as shown in Figure 2.[46]

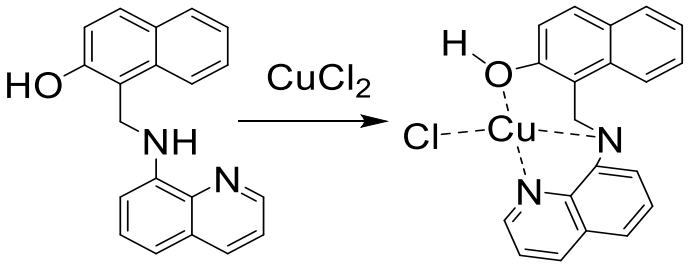

Figure 2: Proposed binding and coordination of quinoline derivative to Cu^{2+} developed by Cai-ling et. al[46]

While PET based fluorescent chemosensors are useful to determine the presence of a metal ion in a sample, Intramolecular Charge Transfer (ICT) based fluorescent chemosensors are a better tool to determine the concentration of the metal ion.

ICT is similar to PET however, rather than being a turn-on response per se, there is a significant shift between the absorption and emission wavelengths and intensities, which means that ratiometric determination is possible.[33] ICT chemosensors, like the one shown in Figure 3, function by containing both an electron donating group, usually a π-conjugated system and an electron withdrawing group, usually a carbonyl group.[33] The polarization within the molecule creates a large dipole moment which leads to a larger Stokes shift. These molecules have traditionally been used for colormetric analyses due to their intense color changes.

Xuan et. al have recently developed an Fe^{2+} chemosensor, shown in Figure 3, which utilizes ICT properties to possibly probe Fe^{2+} in biological processes.[34]

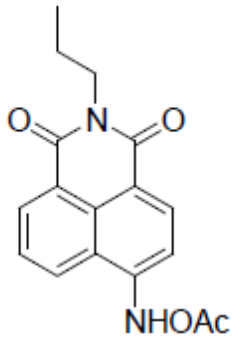

Figure 3: Fluorescent Chemosensor used to detect Fe^{2+} developed by Xuan et. al[34]

A third, more recently, developed type of chemosensor uses the phenomena of Förster Resonance Energy Transfer (FRET).[35] FRET utilizes two fluorophores in close proximity to each other as a donor and acceptor pair. The donor is excited and transfers its energy to the acceptor fluorophore via dipole-dipole interactions.[35] The emission of the donor decreases or becomes quenched, while the emission of the acceptor increases.[35] By measuring the FRET efficiency, the distance between the fluorphores can be determined and is therefore a useful tool in determining protein interactions and other biological processes.[35]

As mentioned, there are several criteria when developing a robust fluorescent chemosensor. The most important criteria are the selectivity for the ion being measured. A selective chemosensor will have less interference from other metal ions and therefore less false-positive measurements. Other important criteria include the

probing sensitivity of the molecule, its stability at various pH, temperature and solvent environments as well as their quantum yields.

A high quantum yield is an important criterion when developing a fluorescent chemosensor. Fluorescence quantum yield is essentially the ratio of the number photons emitted by the fluorophore divided by the number of photons absorbed. In practice, however, since the individual number of photons is difficult to detect without expensive instrumentation and precise calibration, quantum yield is calculated in regards to a reference sample of known emission properties. When choosing the reference fluorophore, it is important to ensure that the emission spectra are similar so that they can be compared.

1.6 Pb^{2+} chemosensors

There have been some recent developments in Pb^{2+} probing with fluorescent chemosensors. Kwon et. al has developed a highly selective chemosensor, shown in Figure 4, which binds to Pb^{2+}.[36] The chemosensor is a Rhodamine B derivative whose mechanism of fluorescence occurs via Chelation Enhanced Fluorescence (CHEF) shown in Figure 5.[36]

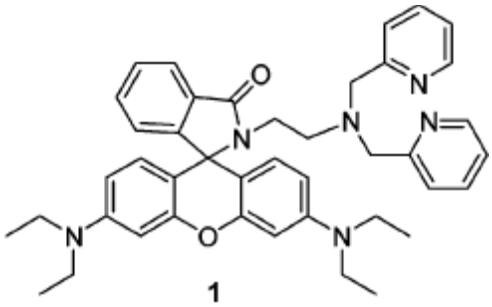

Figure 4: Rhodamine derivative Pb^{2+} chemosensor[36]

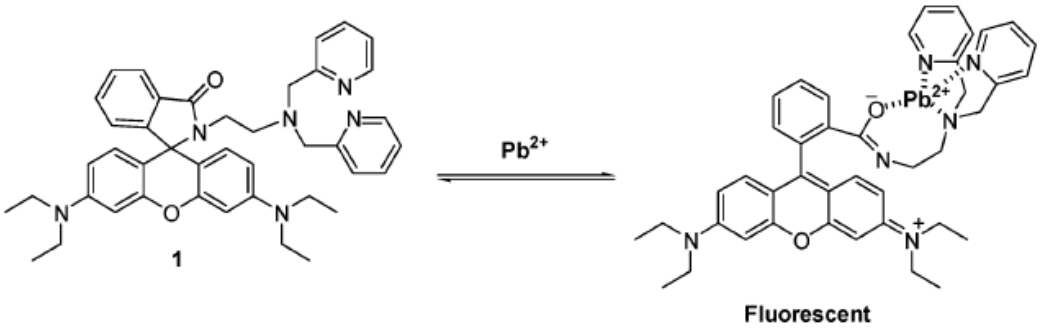

Figure 5: Proposed structure for Rhodamine derivative Pb^{2+} chemosensor complex. Fluorescence occurs after the addition of Pb^{2+} to the previously quenched molecule **1**[36]

This chemosensor shows a 100-fold change in emission upon addition of Pb^{2+}.[36] In addition, the molecule was highly selective for Pb^{2+} ions as compared to perchlorate` salts of Ag^{2+}, Ca^{2+}, Cd^{2+}, Co^{2+}, Cs^{+}, Cu^{2+}, Hg^{2+}, K^{+}, Li^{+}, Mn^{2+}, Na^{+}, Ni^{2+}, Rb^{2+} and Zn^{2+}.[36] While sensitivity was not studied during the experiment, the lowest concentration of lead tested was roughly 400ppb.[36]

1.7 Leadglow

A more versatile method has been recently developed which involves the use of the fluorescent chemosensor, Leadglow, shown in Figure 6, which can selectively bind to Pb^{2+} between pH 4 and 10, is water soluble and has a high quantum yield (0.58) when bound to lead.[21]

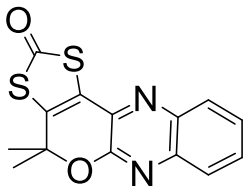

Figure 6: Leadglow molecule developed by Marbella et. al[21]

In addition, this chemosensor shows a concurrent shift in emission intensity based on binding to Pb^{2+} which can be used to quantify lead accurately down to 10ppb and qualitatively indicate the presence of Pb^{2+} via a turn-on response down to 1ppb.[21] Once the leadglow binds to Pb^{2+}, there is a concurrent blue shift in emission wavelength of around 42nm.[21] Leadglow is highly selective for Pb^{2+} when compared to other ions among which include: Fe^{2+}, Cu^{2+}, Zn^{2+}, Mn^{2+} and Sn^{2+} to name a few.[21]

However, as with the other established methods for lead analysis, this method still involves transporting of samples to a laboratory to be tested on an expensive and stationary analytical instrument. Instead a handheld fluorometer which uses the leadglow chemosensor was developed and was used to gather real-time concentration

of Pb^{2+} in aqueous samples. The new device was built with the help of Dr. Corcovilos in the physics department. The device consists of a 3D printed body of PLA plastic, which holds the cuvette, circuitry and optical filters. The device has an excitation wavelength of 390nm and a detector which measures the concurrent emission intensity. Calibration solutions were made with a range of 1ppb-200ppb Pb^{2+} in water to determine the upper and lower limits of detection of the device. A 10μM solution of leadglow in a 2.5% methanol/water in a 20:1 ratio of NEt_4OH:LG was used as the chemosensor solution. The solution was added to the cuvette in the fluorometer and a blank reading was taken with hydrolyzed LG, which will be discussed in Chapter 4. Water samples from local homes were added to the LG sample and the concurrent emission spectra were analyzed. All samples were checked against a HORIBA fluoromax 4 spectrofluorometer for accuracy.

Specific Aims

The study had 3 main goals outlined below:

1. Optimize the Leadglow to binding procedure and develop protocol for testing samples. As part of this aim, several were to be tested such as temperature, base ratio and mixing time to achieve the most favorable conditions for the binding of LG to Pb^{2+}

2. Test a handheld fluorometer prototype to work with Leadglow and derivatives. As part of this aim, test water samples using portable fluorometer and LG and compare to benchtop fluorometer.

3. Synthesize LG derivatives and analyze their lead binding properties.

Chapter 2: Materials/Methods

LG and its naphthalene derivative were synthesized according to the following procedure outlined in section 2.2. The synthesis was confirmed using several spectroscopic methods outlined in section 2.3

2.1 Materials

Diethyl oxalate, (+/-) styrene oxide, 3,4-dihydro-2H-pyran, 2,3-diaminonapthalene, triethylamine (NH_3) , 2-methyl-3-butyn-2-ol and anhydrous magnesium sulfate ($MgSO_4$) were purchased from Alfa Aesar (St. Louis, MO) . Sulfuric acid (H_2SO_4) and mercuric acetate ($Hg(OAc)_2$) were purchased from Fisher Scientific (Pittsburgh, PA). Anhydrous methanol (MeOH) , dry acetone, benzyl chloroformate, Pb^{2+} acetate trihydrate ($Pb(OAc)_2*3H_2O$) , ammonium chloride (NH_4Cl), para-toluenesulfonic acid monohydrate (PTSA) and ortho-phenylenediamine were purchased from Acros. N-butyllithium, trifluoroacetic acid (TFA) , tetraethyl ammonium hydroxide (Et_4NOH) and quinine hemisulfate monohydrate were purchased from Sigma Aldrich (St. Louis, MO). Sodium bicarbonate ($NaHCO_3$) was purchased from VWR (Radnor, PA). Glacial acetic acid was purchased from the Millipore Corporation (Waltham, MA). Hydrochloric acid (HCl) was purchased from the EMD Corporation (Billerica, MA). Silica gel was purchased from Sorbent Technologies (Norcross,GA).

The chemicals purchased were used as bought without further purification. Dry tetrahydrofuran (THF) and dichloromethane (DCM) were obtained from the LC Technologies SP-1 solvent purification system.

Deuterated dimethyl sulfoxide (DMSO) and chloroform ($CDCl_3$) were obtained from Cambridge Isotope Laboratories Inc. (Tewksbury,MA) to be used for Nuclear Magnetic Resonance (NMR) studies.

3.5mL disposable methacrylate UV cuvettes were obtained from Perfector Scientific (Atascadero,CA) and 1cm x 1cm quartz cuvettes were obtained from Starna cells (Atascadero,CA) for fluorescence studies. 1cm x 1cm quartz cuvettes were obtained from Starna cells for UV-vis studies.

2.2 Instrumentation

All infrared spectra were taken on a Nicolet 380 FT-IR spectrometer from the Thermo Electron Corporation and a Perkin Elmer Frontier FT-IR spectrometer. All ^{13}C and ^{1}H NMR spectra were taken on a 500MHz and 400MHz Bruker spectrometer. All fluorescence studies were done on a Horiba Scientific Fluoromax-4 spectrofluorometer, Turner Designs AquaFluor handheld Spectrofluorometer and an in-house manufactured prototype spectrofluorometer. All UV-vis studies were conducted using an Agilent Cary series UV-vis 300 spectrometer. All mass spectrometry studies were conducted on an Agilent Quadrupole- Time of Flight 6530 mass spectrophotometer.

2.3 LG synthetic procedure

Overall, the synthesis of both LG and its naphthalene derivative took seven steps to complete. The first three steps, which are shown below are the same for both LG and the naphthalene derivative.

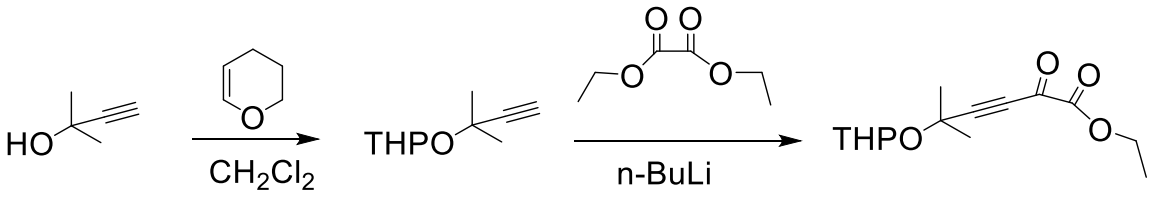

Scheme 1: Synthetic scheme for synthesis of precursor to **1A**

Synthesis of 3-(5-(2- hydroxypropan-2-yl)-2-thioxo-1,3-dithiol-4-yl)- quinoxalin-2(1H)-one

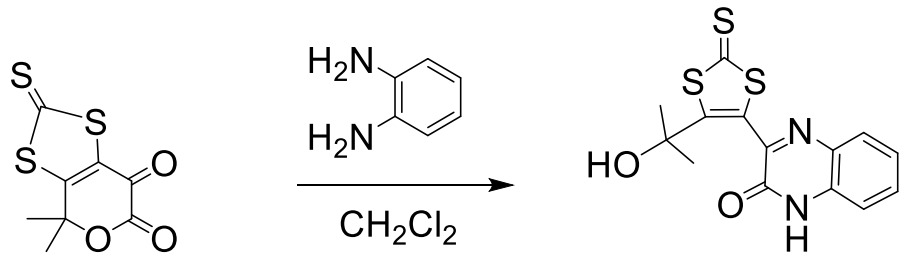

(**1A**) (**2A**)

Scheme 2: Synthetic scheme for condensation reaction of **1A** to yield **2A**

4,4-dimethyl-2-thioxo-4H-[1,3]dithiolo[4,5-c]pyran-2,6,7-dione (**1A**) (1.97g, 8mmol) was dissolved in 20mL DCM. Benzene-1,2-diamine (0.88g, 8 mmol) was added to the

mixture, stirred overnight and a precipitate formed. The reaction mixture was placed in centrifuge tubes and centrifuged for 30 minutes. The reaction mixture was decanted, providing 3-(5-(2- hydroxypropan-2-yl)-2-thioxo-1,3-dithiol-4-yl)- quinoxalin-2(1H)-one (**2A**) as an orange solid. Yield: 1.30 g, 3.90 mmol (48%). H-NMR in DMSO (ppm): δ 12.8 (s,1H), 7.80 (d,1H), 7.63 (t, 1H), 7.36 (t,2H), 1.46(s, 6H). The NMR data shows the condensation reaction was successful due to the addition of a broad peak around 12.8ppm present in compound **2A**. The data matches well with the spectroscopic data reported by Marbella et. al and Diebler.[21,47]

Synthesis of 4,4-dimethyl-4H [1,3] dithiolo [4',5':4,5]pyrano[2,3-b]quinoxaline-2-thione

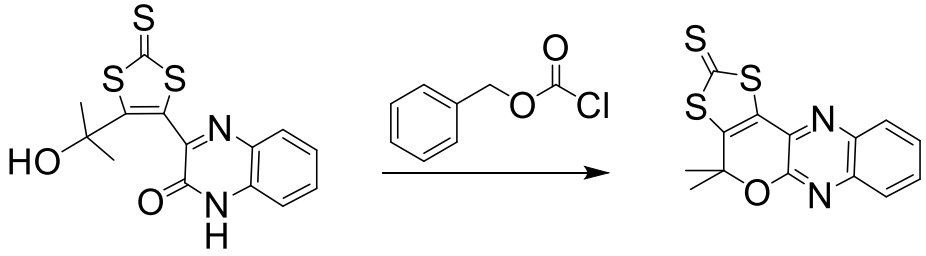

(**2A**) (**3A**)

Scheme 3: Synthetic scheme for ring closure reaction of **2A** to yield **3A**

3-(5-(2- hydroxypropan-2-yl)-2-thioxo-1,3-dithiol-4-yl)- quinoxalin-2(1H)-one (**2A**) (1.23g, 3.66 mmol) was dissolved in 20mL DCM. Benzylchloroformate (1 mL, 7 mmol) was added to the reaction mixture and stirred 15 minutes. Triethylamine (1mL) was

added to the resulting solution was stirred for approximately 2 hours in the dark. The reaction was monitored periodically with TLC (silica, DCM). The mixture was washed with H_2O (3x, 20mL) and the organic layer was saved and dried with $MgSO_4$. The $MgSO_4$ was removed by vacuum filtration and the solvent was removed under reduced pressure to yield impure 4,4-dimethyl-4H [1,3] dithiolo [4',5':4,5]pyrano[2,3-b]quinoxaline-2-thione (**3A**) as a yellow/orange oil. The oil was purified via column chromatography (silica gel 60 Å, DCM eluent) to give pure 4,4-dimethyl-4H [1,3] dithiolo [4',5':4,5]pyrano[2,3-b]quinoxaline-2-thione (**3A**) as a yellow solid. Yield: 1.06 g, 3.33 mmol (91%). H-NMR in $CDCl_3$ (ppm): δ 7.94 (d, 1H), 7.81 (d,1H), 7.66 (t, 1H), 7.59 (t,1H), 1.84(s, 6H). C^{13}-NMR in $CDCl_3$ (ppm): δ 210, 153, 141, 140, 133, 131, 129, 128, 81, 30. The ^{1}H-NMR data shown above shows the loss of the proton shifted to 12.8 ppm from compound **2A**. This verifies the loss of the hydrogen atom on the nitrogen and the subsequent closure of the ring to yield compound **3A**. The ^{1}H-NMR spectrum of compound **3A** is shown in figure 7 with the peaks labeled according to their NMR shifts

The ^{13}C-NMR data shown above was taken to use as a comparison to the proceeding reaction, as the ^{1}H-NMR shifts would show very little difference between compounds **3A** and **4A**.

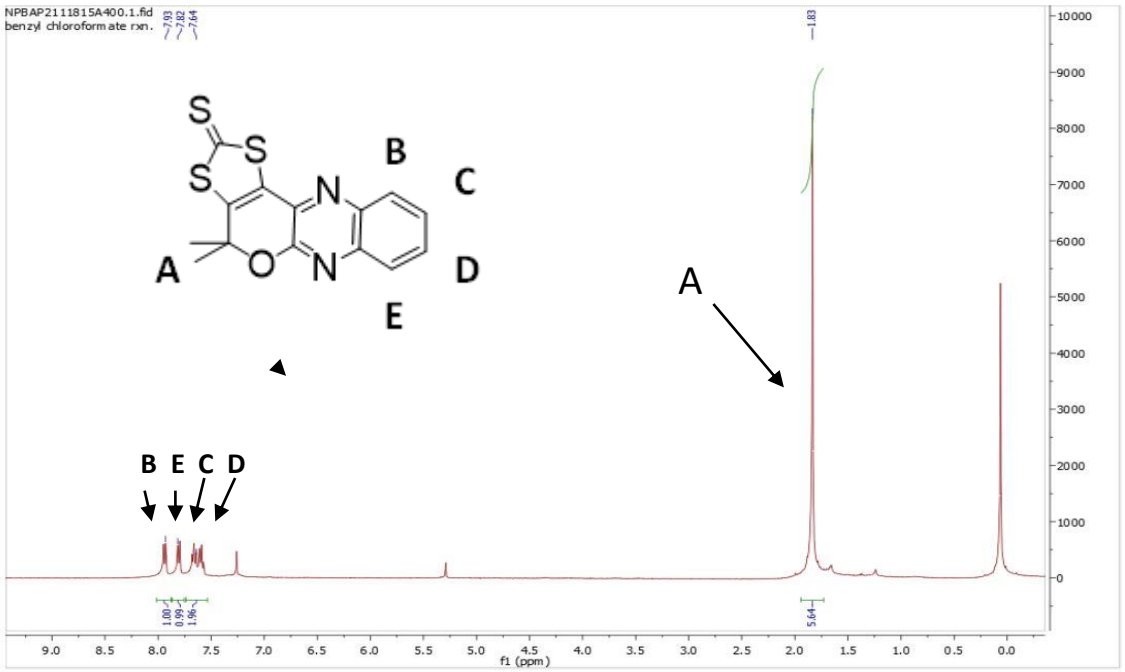

Figure 7: ^{1}H-NMR of **3A** in $CDCl_3$ at room temperature with peaks labeled

Synthesis of LG

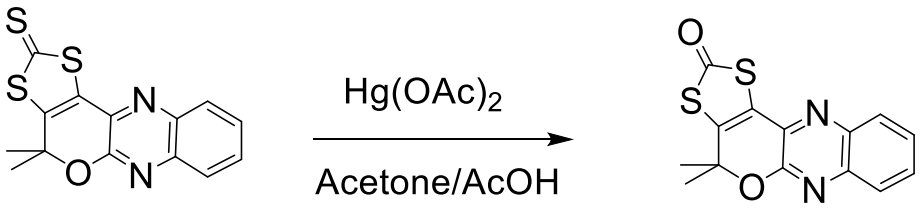

(**3A**) (**4A**)

Scheme 4: Synthetic scheme for oxymercuration reaction of **3A** to yield **4A** (LG)

4-dimethyl-4H [1,3] dithiolo [4',5':4,5]pyrano[2,3-b]quinoxaline-2-thione (**3A**) (0.38g, 1.2mmol) was dissolved in a 40mL mixture of acetone/AcOH (4:1). Mercuric acetate (0.77g, 2.4mmol) was added to the reaction mixture and stirred for about 4 hours in the

dark. The reaction was monitored periodically with TLC (silica, DCM). The mixture was filtered through a celite pad to remove the mercury salts. The resulting solution was washed first with water (3×25 mL) and then with saturated aqueous $NaHCO_3$ (3×25 mL). The organic layer was saved and dried with $MgSO_4$. The $MgSO_4$ was removed by vacuum filtration and the solvent was removed under reduced pressure to afford a pure tan/beige solid as LG. Yield: 40 mg, 0.13 mmol (11%). H-NMR spectrum in $CDCl_3$ (ppm): δ 7.96 (d, 1H), 7.83 (d, 1H), 7.67 (t, 1H), 7.60 (t, 1H), 1.84 (s,6H). ^{13}C-NMR spectrum in $CDCl_3$ (ppm) shown in Figure 8: δ 189, 156, 154, 143, 137, 135, 124, 82, 30. UV-vis in MeOH, λ_{max} (nm) = 256, 367, 386 nm. Fluorescence in MeOH: Excitation = 389 nm, Emission = 423 nm, shown in Figure 9. The overall synthetic scheme for LG is shown in Scheme 5. The ^{1}H-NMR showed no substantial difference between **3A** and **4A**. The ^{13}C-NMR showed a shift of from 210ppm to 389ppm between **3A** and **4A**, verifying the substitution of the C=S for the C=O. The ^{13}C-NMR for **4A** is shown in Figure 8. The fluorescence data shown above for compound **4A** indicates a maximum emission wavelength for a given excitation wavelength. The excitation wavelength was 389nm and the emission range was chosen from 400nm-630nm. The fluorescence spectrum for **4A** is shown in Figure 9. The data matches well with the spectroscopic data reported by Marbella et. al and Diebler.[21,47]

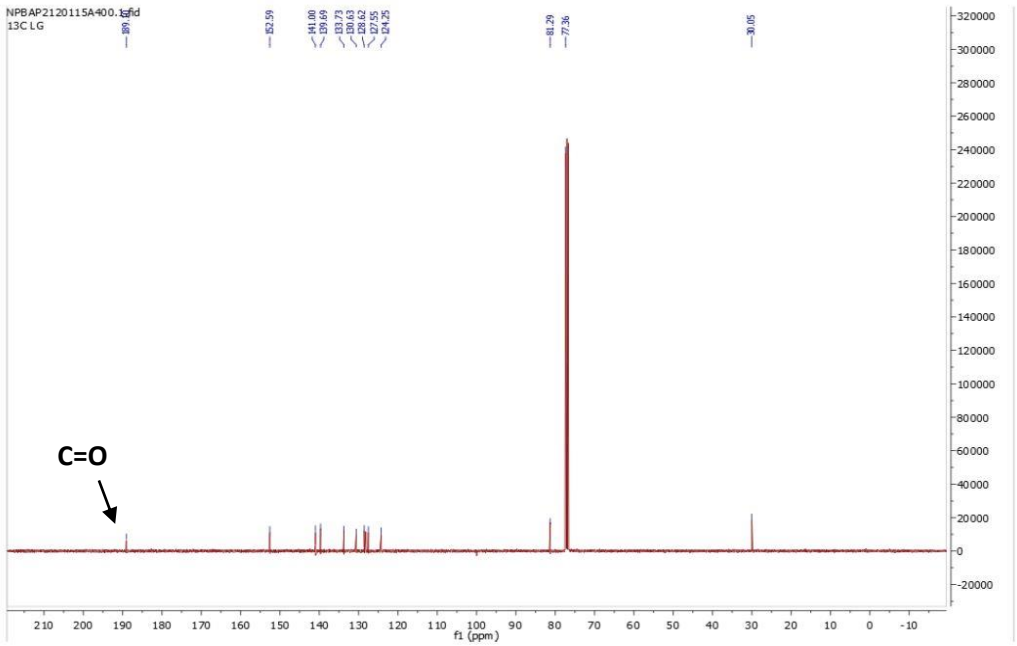

Figure 8: ^{13}C-NMR of **4A** in $CDCl_3$ at room temperature C=O changed at the expense of the C=S peak which appeared at 210ppm

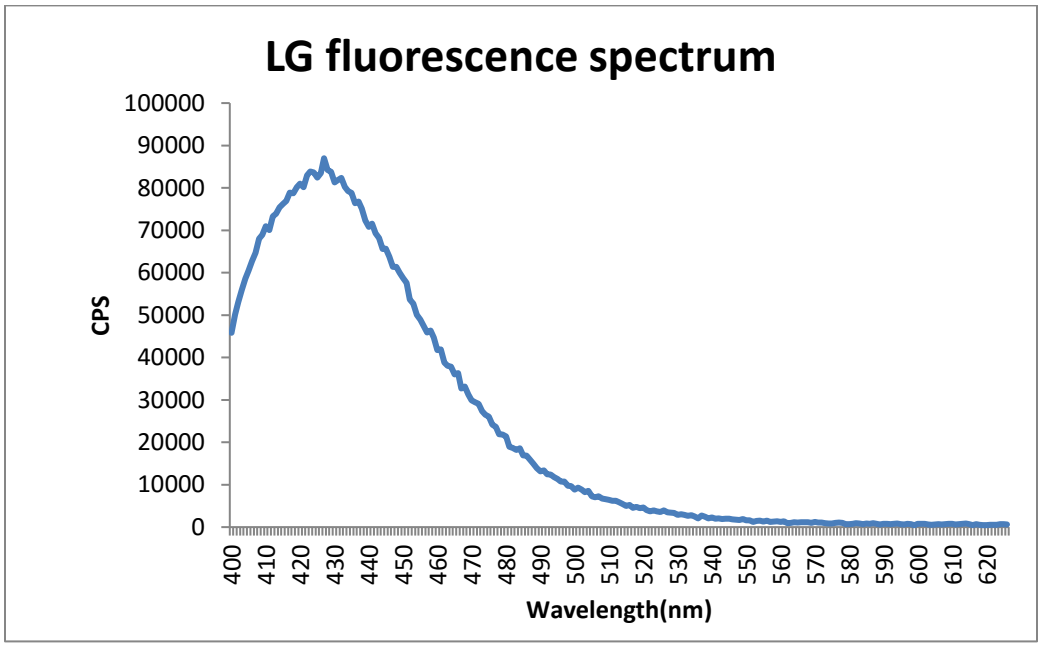

Figure 9: Fluorescence spectrum of **4A** in 2.5% MeOH/H_2O. Excitation: 389nm. Emission maximum: 427nm.

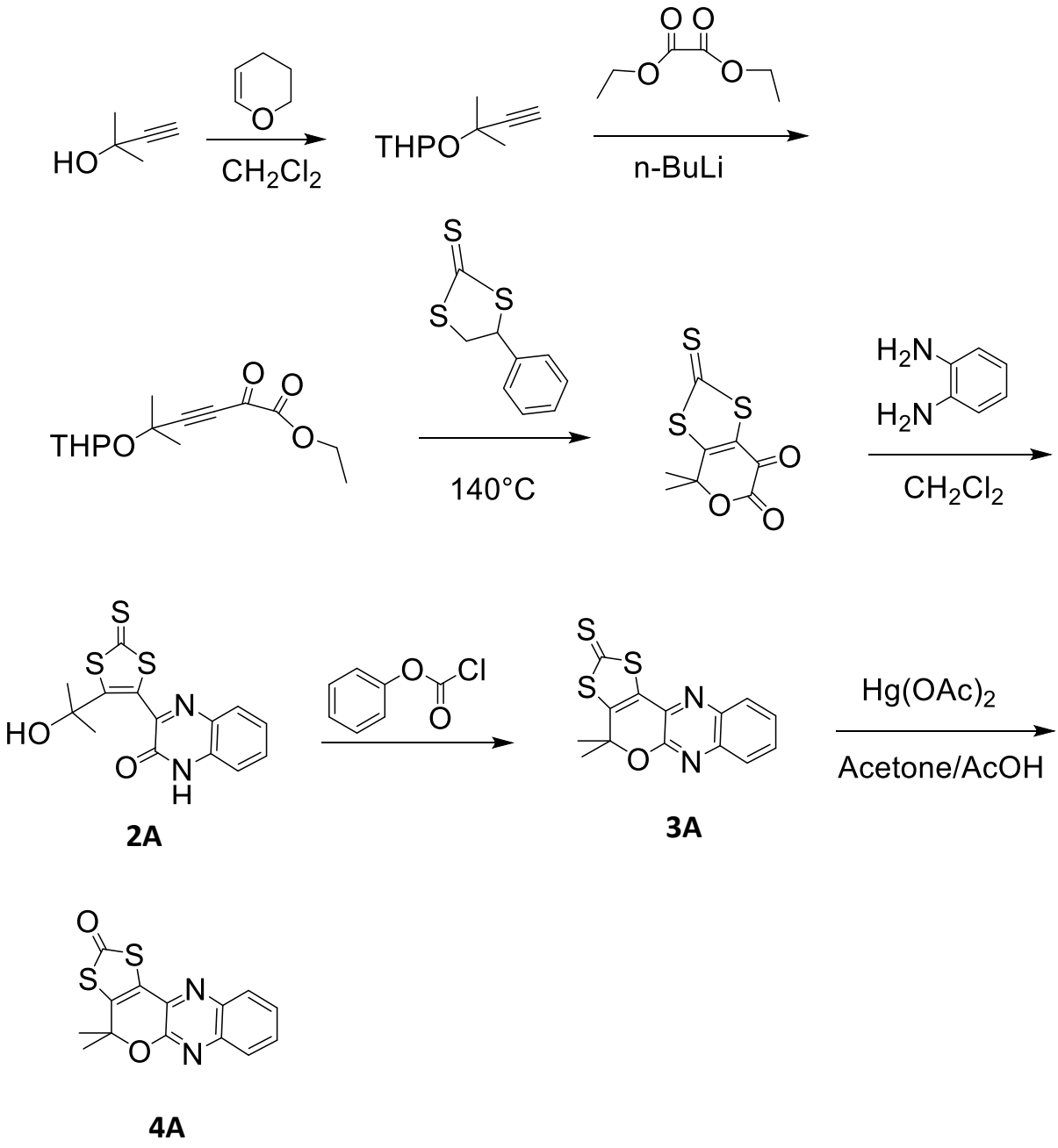

Scheme 5: Complete synthetic scheme for **4A**(LG)

2.4 Naphthalene LG synthetic procedure

Synthesis of 3-(5-(2-hydroxypropan-2-yl)-2- 1,3-dithiol-4-yl)benzo[g]quinoxalin-2(1H)-one

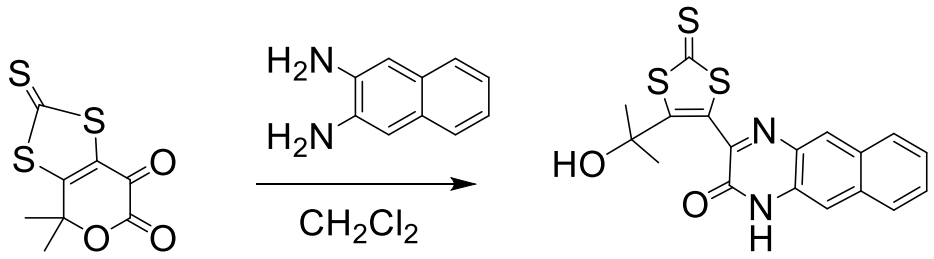

(**1A**) (**1B**)

Scheme 6: Synthetic scheme for condensation reaction of 1**A** to yield **1B**

4,4-dimethyl-2-thioxo-4H-[1,3]dithiolo[4,5-c]pyran-2,6,7-dione (**1A**) (2.12mg, 8.6 mmol) was dissolved in 20mL DCM. Napthalene-2,3-diamine (1.5g, 9.5 mmol) was added to the mixture, the solution was stirred overnight and a precipitate formed. The reaction mixture was placed in centrifuge tubes and centrifuged for 30 minutes. The liquid was decanted off, affording 3-(5-(2-hydroxypropan-2-yl)-2- 1,3-dithiol-4-yl)benzo[g]quinoxalin-2(1H)-one (**1B**) as a brown-yellow solid. Yield 1.1 g, 2.85 mmol (38%). H-NMR in DMSO (ppm): δ 8.47 (s,1H), 8.10 (d, 1H), 7.97 (d, 1H), 7.69 (s, 1H), 7.59 (t, 1H), 7.49 (t, 1H), 1.50 (s, 6H). The data matches well with the spectroscopic data reported by Marbella et. al and Diebler.[21,47]

Synthesis of 4,4-dimethyl-4H-[1,3] dithiolo [4',5':4,5] pyrano[2,3-b]benzo[g]quinoxaline-2-thione

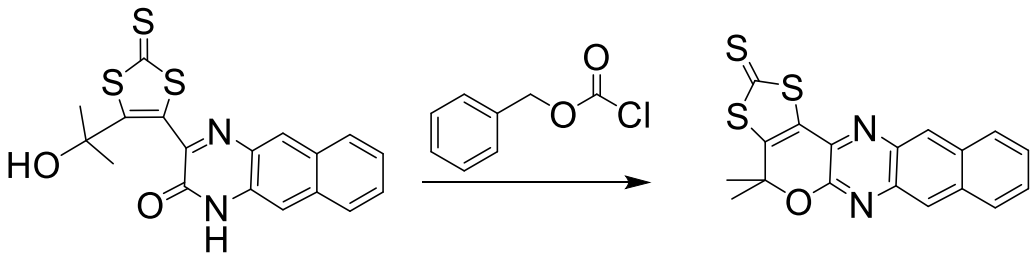

(**1B**) (**2B**)

Scheme 7: Synthetic scheme for ring closure reaction of **1B** to yield **2B**

3-(5-(2-hydroxypropan-2-yl)-2-thioxo-1,3-dithiol-4-yl)benzo[g]quinoxalin-2(1H)-one (**2B**) (1.1g, 2.85 mmol) was dissolved in 25mL DCM. Benzylchloroformate (20mL, 130 mmol) was added to the mixture and stirred for 15 minutes. Triethylamine (20mL) was added and the resulting solution was stirred for about 3 hours. The solution was washed with H_2O (3x20mL), the organic layer kept and dried with $MgSO_4$ overnight. The $MgSO_4$ was vacuum filtrated off and the solvent was removed under reduced pressure to yield oil. The crude oil was purified by column chromatography (silica gel 60 Å, DCM as eluent) to give pure 4,4-dimethyl-4H-[1,3] dithiolo [4',5':4,5] pyrano[2,3-β]benzo[γ]quinoxaline-2-thione (**2B**) as a yellow solid. Yield: 200 mg, 0.54 mmol (19%). H-NMR spectrum in $CDCl_3$ (ppm): δ 8.57 (s, 1H), 8.34 (s, 1H), 8.06 (m, 2H), 7.57 (m, 2H),

1.90 (s, 6H). The data matches well with the spectroscopic data reported by Marbella et. al and Diebler.[21,47]

The ^{1}H-NMR data shown above indicates the transition from four distinct proton splitting patterns on the terminal phenyl group in **1B** to two distinct proton splitting patterns on the terminal phenyl group in **2B**. This verifies the synthesis of a more symmetric compound and the subsequent closure of the ring to yield compound **2B**.

Synthesis of Napthalene LG

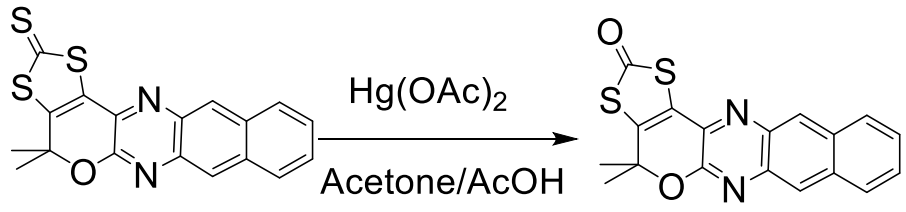

(**2B**) (**3B**)

Scheme 8: Synthetic scheme for oxymercuration reaction of **2B** to yield **3B**

4,4- dimethyl-4H-[1,3]dithiolo[4',5':4,5]pyrano[2,3-b]benzo[g]quinoxaline-2-thione (**2B**) (152 mg, 0.48 mmol) was dissolved in a 40mL mixture of acetone/AcOH (4:1). Mercuric acetate (0.50g, 1.57 mmol) was added to the reaction mixture and stirred for about 4 hours in the dark. The reaction was monitored periodically with TLC (silica, DCM). The mixture was filtered through a celite pad to remove the mercury salts. The resulting solution was washed first with water (3×25 mL) and then with saturated aqueous

$NaHCO_3$ (3×25 mL). The organic layer was saved and dried over $MgSO_4$. The $MgSO_4$ was vacuum filtered off and the solvent was removed under reduced pressure to afford pure light yellow solid 4,4-dimethyl-4H [1,3] dithiolo [4',5':4,5]pyrano[2,3-b]benzo[g] quinoxaline- 2-one (**3B**) as Napthalene LG. Yield: 130mg, 0.37 mmol (89%). H- NMR spectrum in $CDCl_3$ (ppm): δ 8.54 (s, 1H), 8.31 (s, 1H), 8.03 (t, 2H), 7.53 (m, 2H), 1.88 (s, 6H). UV-vis in MeOH, λ_{max} (nm) = 280, 320, 380, 396 nm, shown in Figure 10. Fluorescence in MeOH: Excitation = 389 nm. Emission = 527 nm, shown in Figure 11. The overall synthetic scheme for Napthalene LG is shown in Scheme 9. The ^{1}H-NMR showed no substantial difference between **2B** and **3B**. The UV-vis data above for compound **3B** showed several wavelengths where the absorbance of the compound was maximized. The UV-vis spectrum is shown in Figure 10. The fluorescence data shown above for compound **3B** indicates a maximum emission wavelength for a given excitation wavelength. The excitation wavelength was 389nm and the emission range was chosen from 450nm-700nm. From the spectrum, it is evident that there is a large Stokes shift between the excitation and emission wavelengths, and therefore could be a better chemosensor to test Pb^{2+} when compared to LG due to less of an overlap between the excitation and emission spectra. The fluorescence spectrum for **3B** is shown in Figure 11. The data matches well with the spectroscopic data reported by Marbella et. al and Diebler.[21,47]

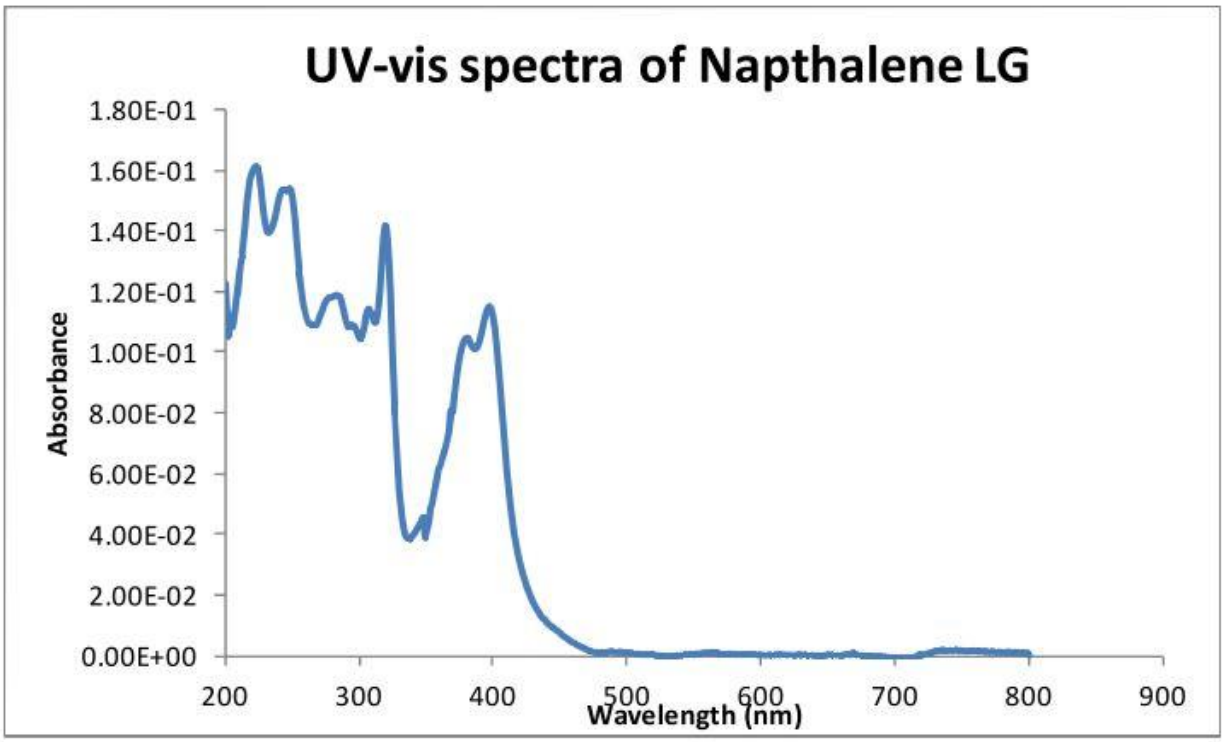

Figure 10: UV-vis spectrum of diluted **3B** in 50% acetone/water

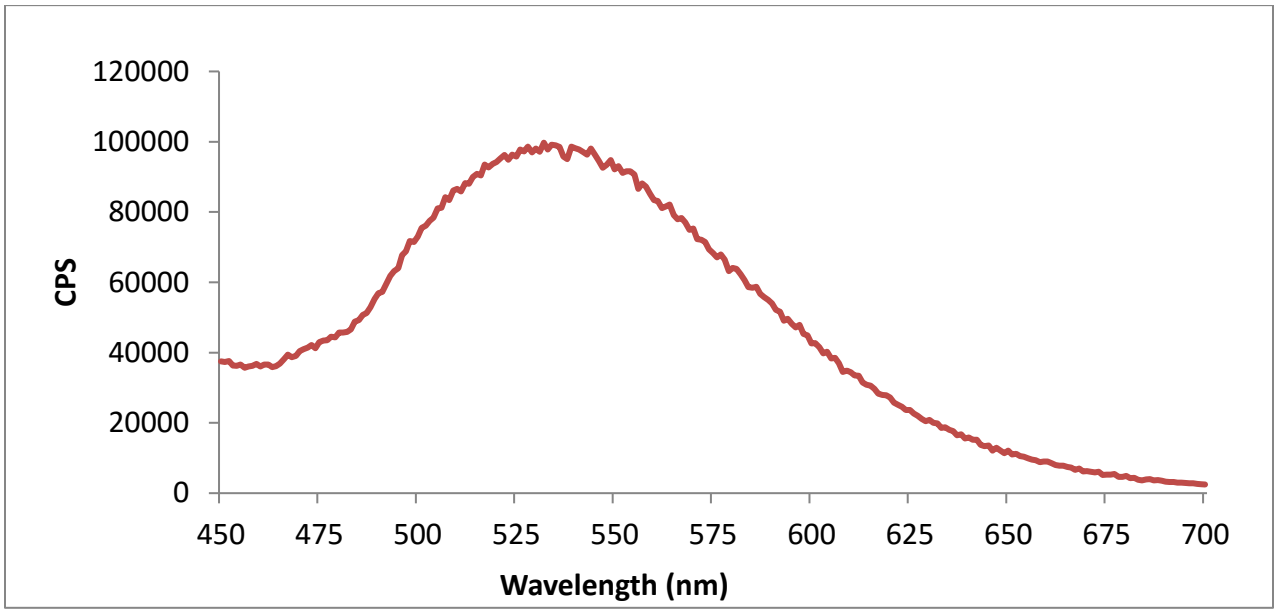

Figure 11: Fluorescence spectrum of **3B** in 50% acetone/water. Excitation: 389nm. Emission maximum: 527nm

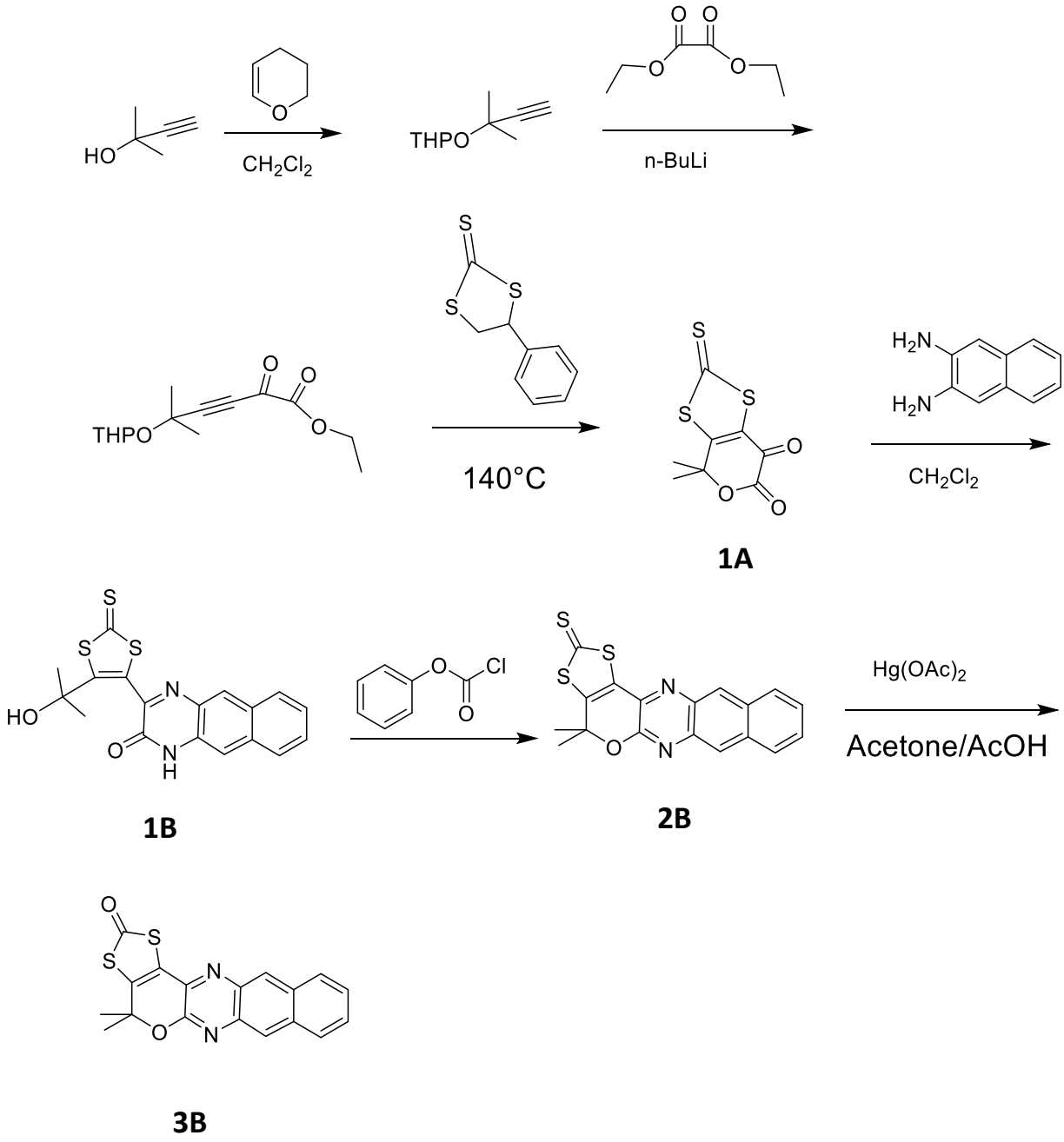

Scheme 9: Complete synthetic scheme for **3B** (Napthalene LG)

Chapter 3: Portable fluorometer

3.1 Commercially available device

Before the lead binding properties of LG was tested on the prototype handheld fluorometer it was first tested on a commercially available device. A handheld fluorometer was purchased from Turner Designs called an Aquafluor handheld fluorometer. The device was ordered fitted with a 375nm LED light and a filter with an emission detection range of greater than 420nm. The LG was tested with lead on the device for which the calibration curve is shown in Figure 12.

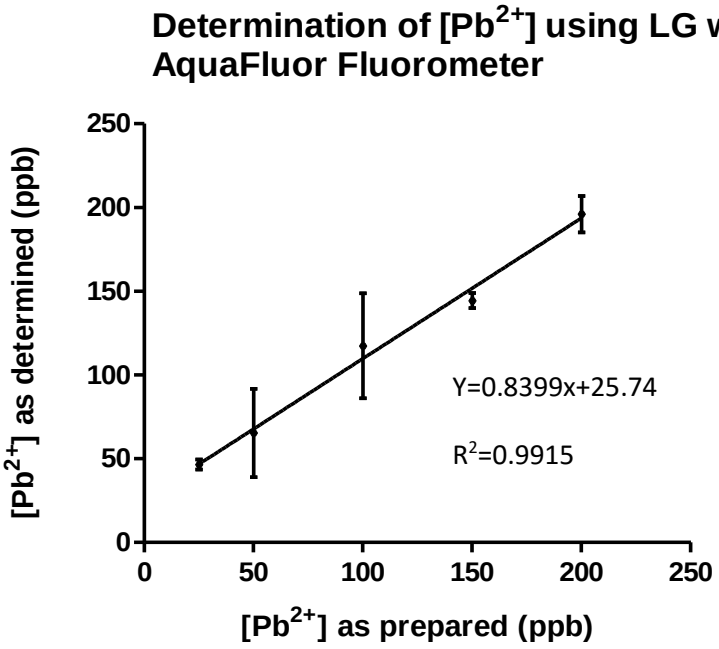

Figure 12: Aquafluor spectrofluorometer lead calibration curve using LG. Excitation: 375nm. Error bars calculated by Graphpad Prism software

The lowest lead concentration quantified was 25ppb. Any concentrations lower than 25ppb gave the same reading as the blank, so therefore we could not determine a lead value lower than 25ppb using this device. The data shows that 25ppb standard was detected as 50ppb on the device. This could be because the LED at 375nm fitted into the device was different than the optimal excitation wavelength of 389nm for LG. In addition, the large error for the 50ppb and 100ppb standard samples signify this as a poor method to determine lead concentration, as these values are indterminable from the 25ppb value. Therefore we thought we could achieve better sensitivity if we developed a handheld fluorometer in-house.

3.2 Internally developed device

A couple iterations of the prototype fluorometers were developed. The first iteration, shown in Figure 13 has a similar engineering design to Horiba Fluoromax 4 bench top Spectrofluorometer, albeit on a smaller scale and with broader ranges for the excitation and emission wavelengths, or in other words more scattering, due to less precise filters and lack of monochromators on the device.[38]

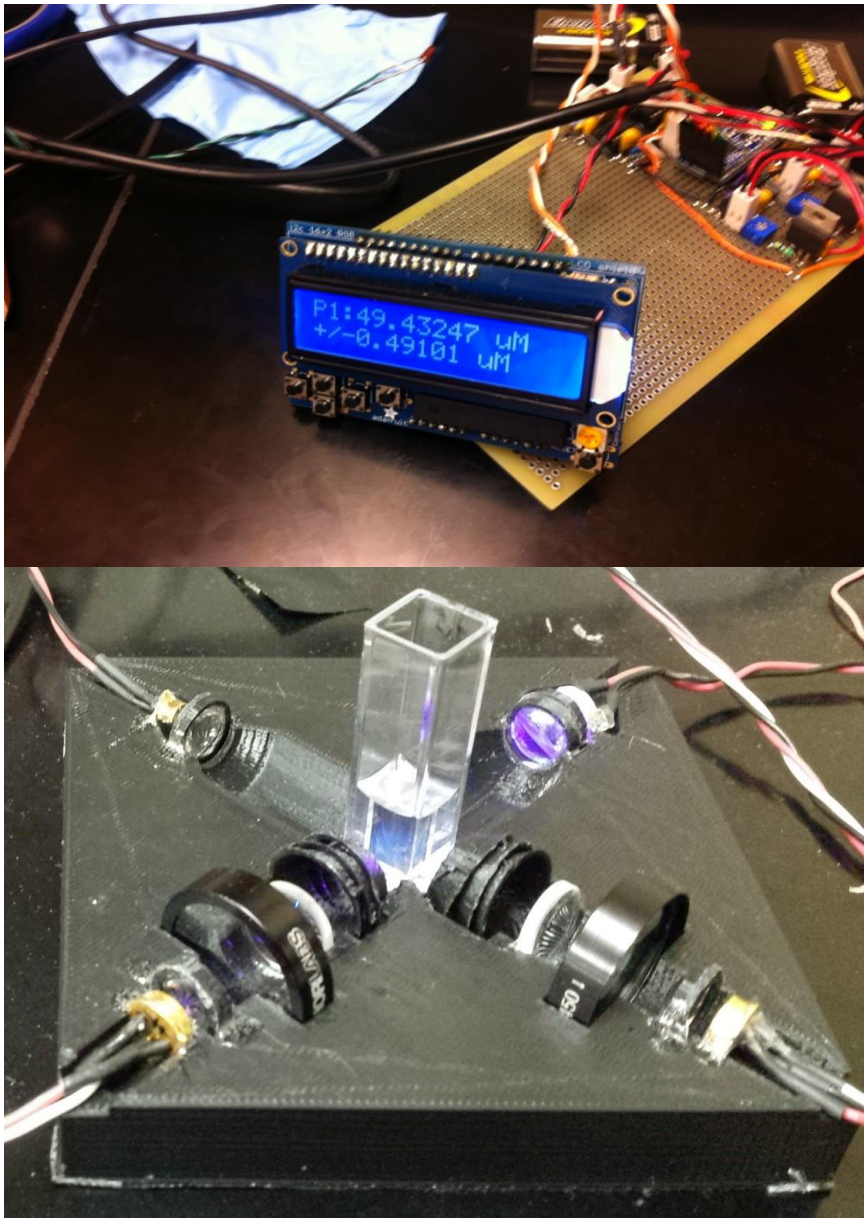

Figure 13: Prototype spectrofluorometer interface and device

A second iteration of the hand held fluorometer was designed in order to reduce background noise and achieve a better spectral resolution by incorporating optical filters better matched to LG and a new optical layout. The schematic for the second iteration of the prototype fluorometer is shown in Figure 14.

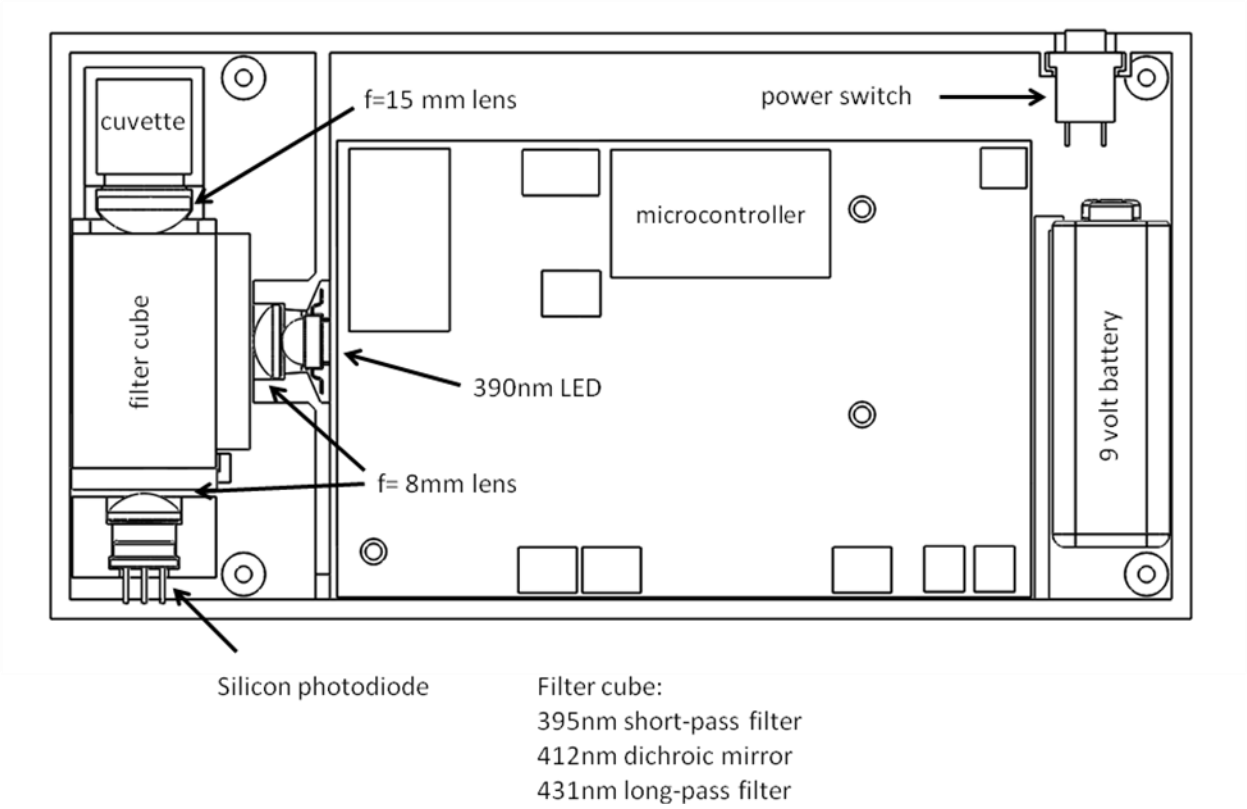

Figure 14: Schematic of prototype fluorometer

The main optical components of the prototype are the LED light, short-pass excitation filter, long-pass emission filter and a dichroic mirror to combine both light paths. The LED light will emit light into the filter cube, where the short-pass filter will filter out any greater than 395nm to ensure that the only light emitted from the sample is due to fluorescence. The light that goes through the short-pass filter will then enter the sample chamber where it will excite the sample. From there, the emitted light will go back to the filter cube where a dichroic mirror will reflect light which is less than 412nm while transmitting light which is greater than 412nm. . The transmitted light will pass

through a long-pass filter which will only allow light above 431nm through to the detector.[39] Once the filtered light leaves the cube it will hit a photodiode which converts the incident light intensity to a voltage. The higher the light intensity the higher the voltage and therefore the greater the fluorescence signal. Two photographs of the device are shown in Figure 15.

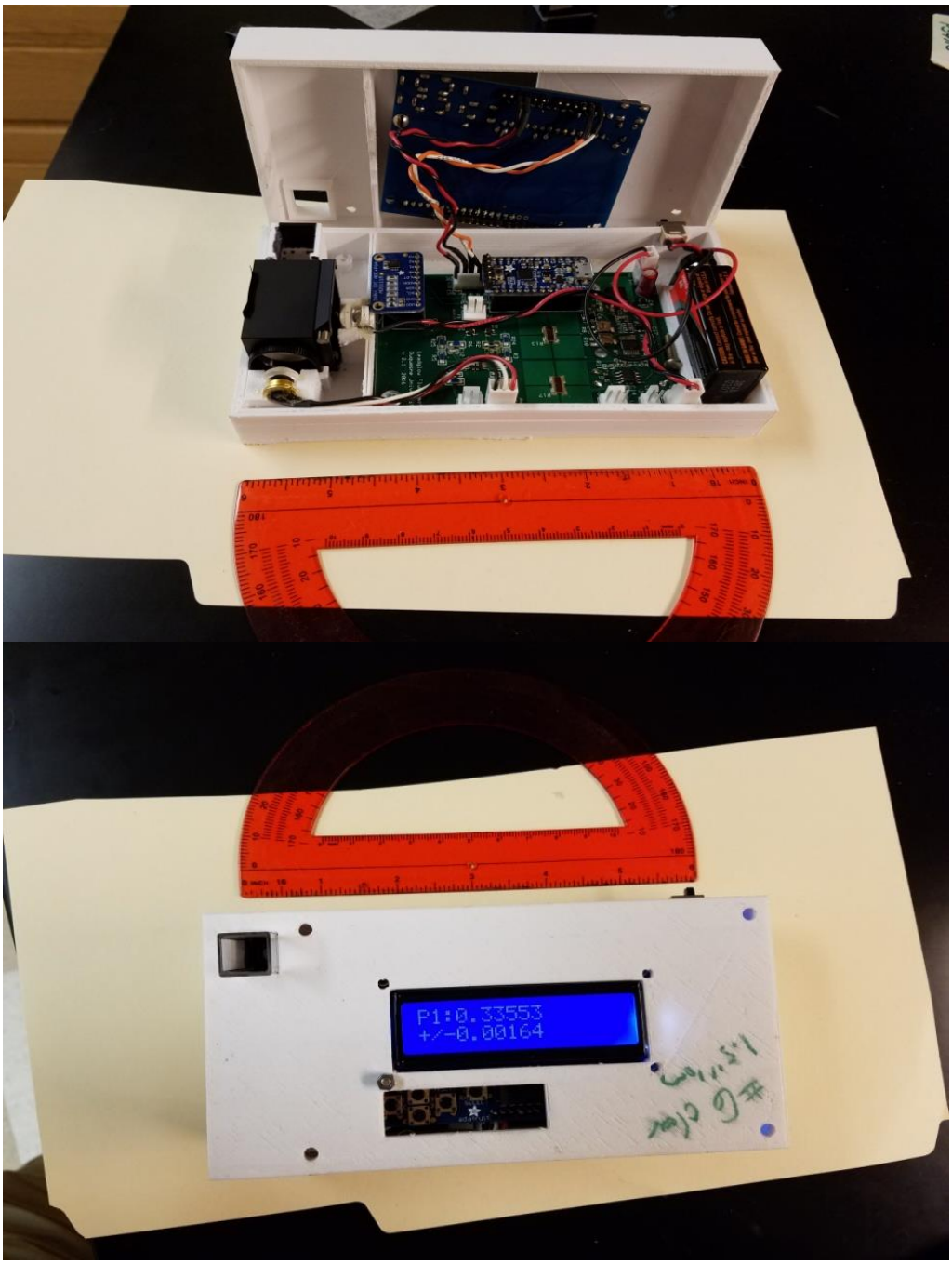

Figure 15: Second iteration portable fluorometer with optical components and frame

3.3 Quantum yield

The quantum yield of both the unbound LG and the Napthalene derivative were calculated in reference to Quinine hemisulfate in accordance to Equation 2 shown below, where Φ_x is the quantum yield of the sample, Φ_{ST} is the quantum yield of the reference sample, $\mathbf{Grad}_x$ is the gradient of the integration of the fluorescence spectrum vs absorbance spectrum of the sample, $\mathbf{Grad}_{ST}$ is the gradient of the integration of the fluorescence spectrum vs absorbance spectrum of the reference sample, $\boldsymbol{\eta}_x$ is the refractive index of the solvent which the sample is in and $\boldsymbol{\eta}_{ST}$ is the refractive index of the solvent the reference is in.

$$\boldsymbol{\phi}_X = \boldsymbol{\phi}_{ST}\left(\frac{\mathbf{Grad}_X}{\mathbf{Grad}_{ST}}\right)\left(\frac{\boldsymbol{\eta}_x^2}{\boldsymbol{\eta}_{ST}^2}\right)$$

Equation 2

Quinine hemisulfate was chosen as the reference sample since it had a similar absorption and fluorescence spectrum, including optimal excitation wavelength when compared to the free LG. The graphs of the gradients of both LG and its naphthalene derivative are shown in Figure 16. The quantum yields were calculated to be 0.12 for LG and 0.29 for the naphthalene derivative.

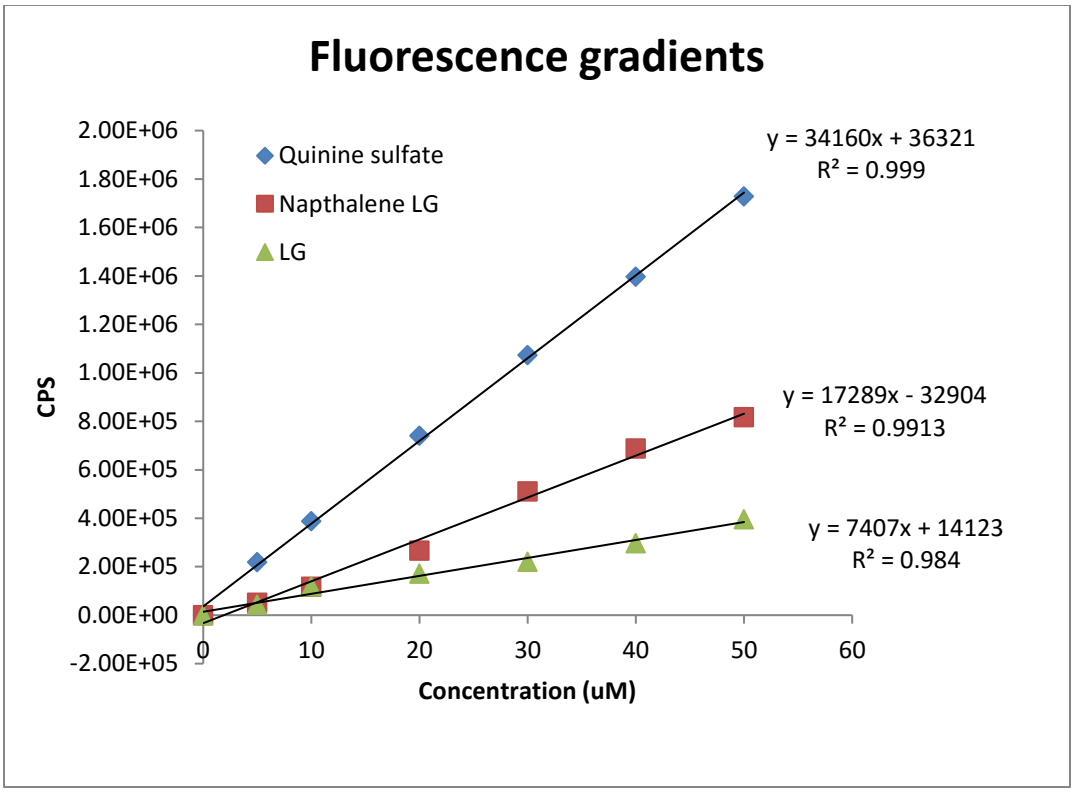

Figure 16: Fluorescence gradients of LG and Napthalene LG in reference to quinine hemisulfate. Excitation: 389nm for LG and Napthalene LG, 350nm for Quinine Sulfate. Emission maximum: 427nm for LG, 527nm for Napthalene LG and 450nm for Quinine Sulfate.

The data shows that there seems to be a background signal as the y intercept is not zero. This could be due to overlap between the excitation and emission spectrum.

Chapter 4: Binding optimization

4.1 LG hydrolysis and binding

LG by itself, known as **free** LG, cannot bind to lead as addition of as the electron rich sulfur atoms are already bound to the carbonyl group. Therefore, an additional step is needed to remove the carbonyl group and allow the sulfur atoms to bind to lead. This is achieved with the addition of a base, termed as the hydrolysis step. Once the base is added, under the optimal conditions specified later in the chapter, the free LG is considered **hydrolyzed** LG**.** In the hydrolysis step, the fluorescent signal from the free LG is minimized to reduce any background interference from the compound. Pb^{2+}, dissolved in an aqueous media, can now freely be complexed by the LG and once it has done so, it is indicated as **bound** LG. Subsequent addition of Pb^{2+} to LG, even in low concentrations will yield an increase in fluorescent signal, up to a certain point where Pb^{2+} exceeds LG in the solution. When this happens, the signal is considered saturated as excess of Pb^{2+} will not lead to a substantial increase in fluorescent signal. While the exact binding method of Pb^{2+} to LG in the presence of a base is not known, a theorized method is shown in Figure 17.

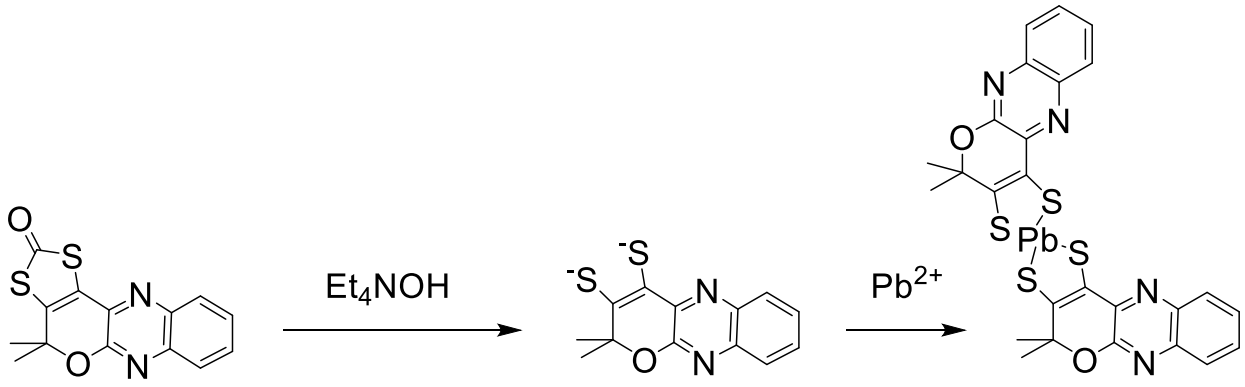

Figure 17: Proposed hydrolysis and complexation of LG to Pb^{2+}

Once the sulfur atoms are exposed, the lead possibly coordinates to the LG in a 2 LG: 1 Pb^{2+} ratio.[21] However, in order to maximize the binding of the lead to LG several criteria need to be optimized. These criteria include the ratio of the base to LG, the mixing time between them and the temperature.

4.2 Base ratios experiment

The binding protocol and procedure of Pb^{2+} to leadglow was also optimized. The first step in the optimization was to determine an optimal base to leadglow ratio to ensure that the maximum amount of leadglow was hydrolyzed. If the base ratio was too low, the LG would not be fully hydrolyzed and there would be a high background signal from the excess free LG. If the base ratio was too high, any lead were present in the solution would be precipitated out as $Pb(OH)_2$ and would not be available for binding to the LG molecule. To test this theory an experiment was conducted with different ratios of base. For this experiment, all the vortexing was kept constant at 30

minutes per sample. Figure 18 shows the fluorescence spectrum of different base to leadglow ratios.

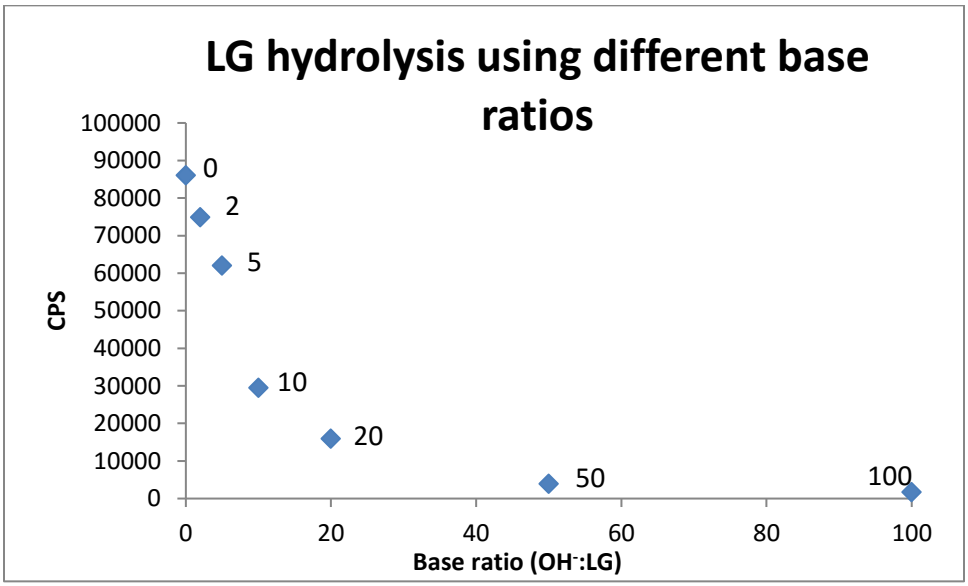

Figure 18: Ratio of OH^- to LG dissolved in 2.5% MeOH/H_2O fluorescence intensity curve. Excitation 389nm. Emission maximum: 427nm

As seen in the Figure above, a 100:1 base to LG ratio would theoretically be best because it hydrolyzed the largest amount of LG. The K_{sp} calculation in Equation 3 suggested an optimal base to LG ratio of 20:1 where the most LG would be hydrolyzed while not precipitating out much of the Pb^{2+}.

$$Pb(OH)_2(s) \longrightarrow Pb^{2+}(aq)+2OH^-$$

$$K_{sp} = \left[Pb^{2+} \right] \left[OH^- \right]^2$$

Equation 3

The solubility of a salt in a solution is based on its solubility product equilibrium constant. At 25 °C the equilibrium K_{sp} for Pb^{2+} hydroxide is 1.2×10^{-15}. Above this value, the precipitate is more likely to form, meaning that the base ratio is not optimal to use. Figure 19 shows a graph of the calculated Ksp values with different base ratios, assuming the same concentration of lead. The ideal base ratio would be close to the Ksp value but also hydrolyzes the most amount of LG.

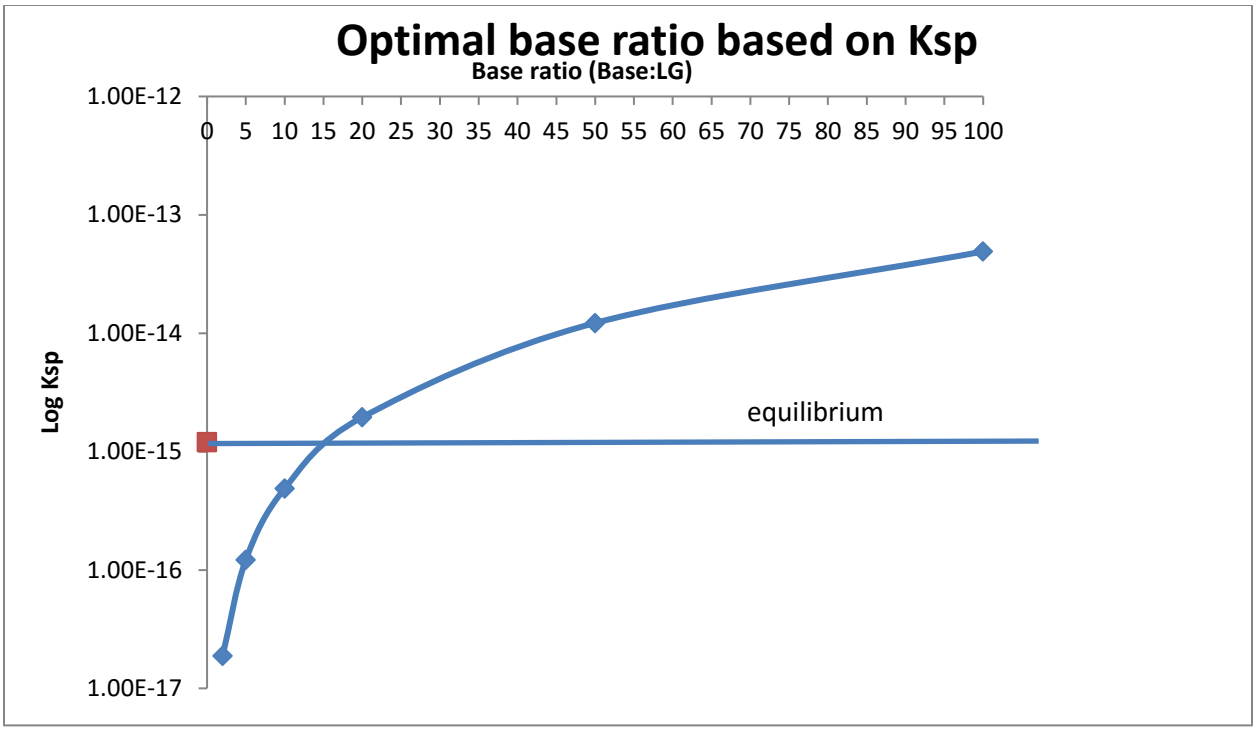

Figure 19: Calculated Ksp values based on assuming 10ppb Pb^{2+} in each sample and changing base to LG ratios

4.3 LG temperature experiment

In addition to the base ratio, we wanted to see what effect temperature would have on the emission of LG. The temperature was kept at a constant 60 °C during a mixing time of 30 minutes for each sample. The results of the experiment are shown in Figure 20.

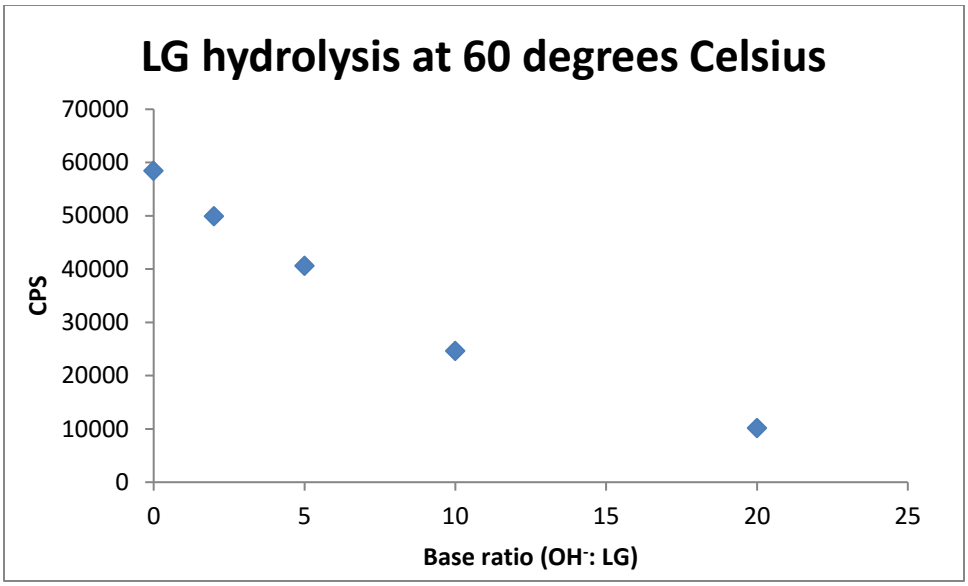

Figure 20: Fluorescence intensity of LG dissolved in 2.5% MeOH/H_2O at 60 °C using different base ratios. Excitation: 389nm. Emission maximum: 427nm

According to the results, there was a decrease in emission intensity for all the base ratios when heated to 60 °C. However, both the 10:1 and 20:1 base ratios showed very little difference when compared to the room temperature graph in Figure 18.

4.4 LG time experiment

Once an optimal base ratio was determined based on the Ksp calculation and emission intensity graph in Figure 18, then an acceptable mixing time needed to be established. For the experiment the 20:1 base to leadglow ratio was kept constant between the samples with only the mixing time being adjusted. The results of the experiment are shown in Figure 21.

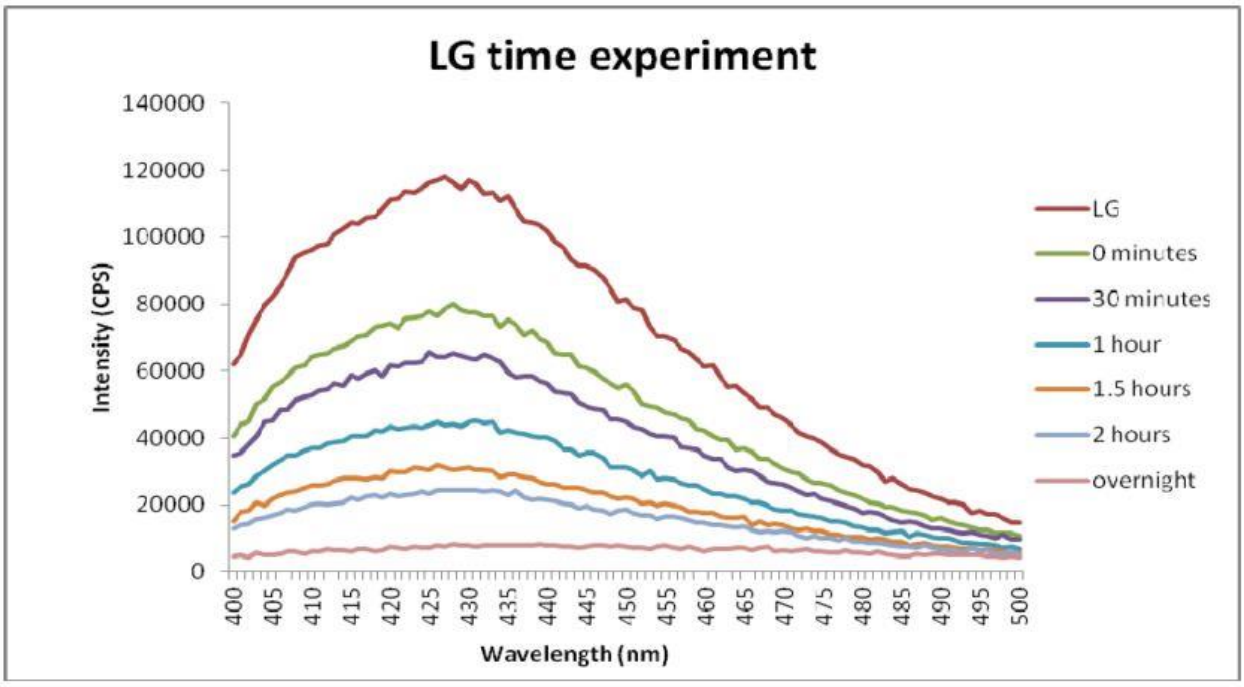

Figure 21: LG emission spectrum with different mixing times

According to the experiment, the longer the LG is mixed, the lower the emission signal will be and therefore the more hydrolyzed LG will be available for binding to Pb^{2+}. Ideally, then, an overnight hydrolysis of the LG would yield the biggest drop in emission, however due to the practicability of using LG in a portable field setting, a mixing time of 30 minutes was chosen. However, due to the drifting of the background signal over time, the calculated lead concentrations will be higher than they really are, as the background has changed. This time was also chosen as the majority of the leadglow was hydrolyzed at that point.

4.5 LG calibration protocol

Once the binding of LG to Pb^{2+} was optimizied the following protocol and procedure was developed. The protocol used to test the LG was developed according to the following procedure.

1. **Base Solution:** Add 10uL 2.7M Et_4NOH (40% in water) stock solution to a 10mL volumetric flask and bring to volume with 2.5% MeOH to give a $2.7x10^{-3}$ M solution
2. **Lead solution:** Dissolve 10mg ($4.8x10^{-5}$ mol Pb^{2+}) in a 10mL volumetric flask and bring to volume with 2.5% MeOH to give a 1ppt solution. Dilute 1000x by adding 10uL of the stock solution to a 10mL volumetric flask and bring to volume with 2.5% MeOH to give a 1ppm Pb^{2+} solution.
3. **Leadglow solution:** Completely dissolve 3mg (10^{-5} mol) LG in a 100mL volumetric flask in 2.5mL methanol, and make up the volume with ultrapure H_2O to give a 10^{-4} M solution. If any solids are still present, filter them off.

Experimental Procedure

1. Add 150uL ($1.5x10^{-8}$ mol) leadglow to dark Eppendorf tubes as per number of samples. Each tube is then used for sample preparation as follows.
2. **Blank:** 150uL leadglow+ 112uL base (20:1 base:LG) + 1238uL 2.5% MeOH

Lead Solutions:

10ppb: 150uL leadglow+ 112uL base (20:1 base:LG) + 1223uL 2.5% MeOH+15uL 1ppm Pb^{2+}

20ppb: 150uL leadglow+ 112uL base (20:1 base:LG) + 1208uL 2.5% MeOH+30uL 1ppm Pb^{2+}

30ppb: 150uL leadglow+ 112uL base (20:1 base:LG) + 1193uL 2.5% MeOH+45uL 1ppm Pb^{2+}

40ppb: 150uL leadglow+ 112uL base (20:1 base:LG) + 1178uL 2.5% MeOH+60uL 1ppm Pb^{2+}

50ppb: 150uL leadglow+ 112uL base (20:1 base:LG) + 1163uL 2.5% MeOH+75uL 1ppm Pb^{2+}

100ppb: 150uL leadglow+ 112uL base (20:1 base:LG) + 1088uL 2.5% MeOH+150uL 1ppm Pb^{2+}

3. After making all the solutions vortex for 30 minutes at RT then transfer 1.2mL of the vortexed solution to a 1cmx1cm methacrylate plastic cuvette and take reading on either bench top or portable fluorometer

4.6 Napthalene LG solubility

The lead binding properties of Napthalene LG were also studied. Since Napthalene LG is more non-polar than LG, methanol was not a suitable solvent to use

to dissolve the compound in. A qualitative approach was taken to identify a suitable solvent that the Napthalene LG could be dissolved in, shown in Table 2.

Solvent	**Soluble**
Ethyl Acetate	Yes
Dichloromethane	Yes
Acetone	Yes
Methanol	No
Ethanol	No
Isoproponal	No
n-hexanes	No

Table 2: Qualitative solubility test of Napthalene LG

Of the three solvents which Napthalene LG was soluble in, only acetone was the viable option due to it being less of a health and environmental risk hazard when compared to ethyl acetate and dichloromethane. However, due to acetone's incompatibility with plastic cuvettes due to etching, a suitable ratio of acetone to water needed to be determined in order for the maximum amount of Napthalene LG to be dissolved without etching to occur in the cuvette. In addition, quartz cuvettes are too

expensive to be used in a field setting, and they need to carefully be washed after use with acid to remove any trace metals.

4.7 Napthalene LG lead binding

After the solubility of the napthalene LG was determined, the lead binding properties of the molecule was also determined. The same testing protocol and experimental procedure were used as was outlined in chapter 4. Figure 22 shows the calibration curve of Napthalene LG with Pb^{2+}.

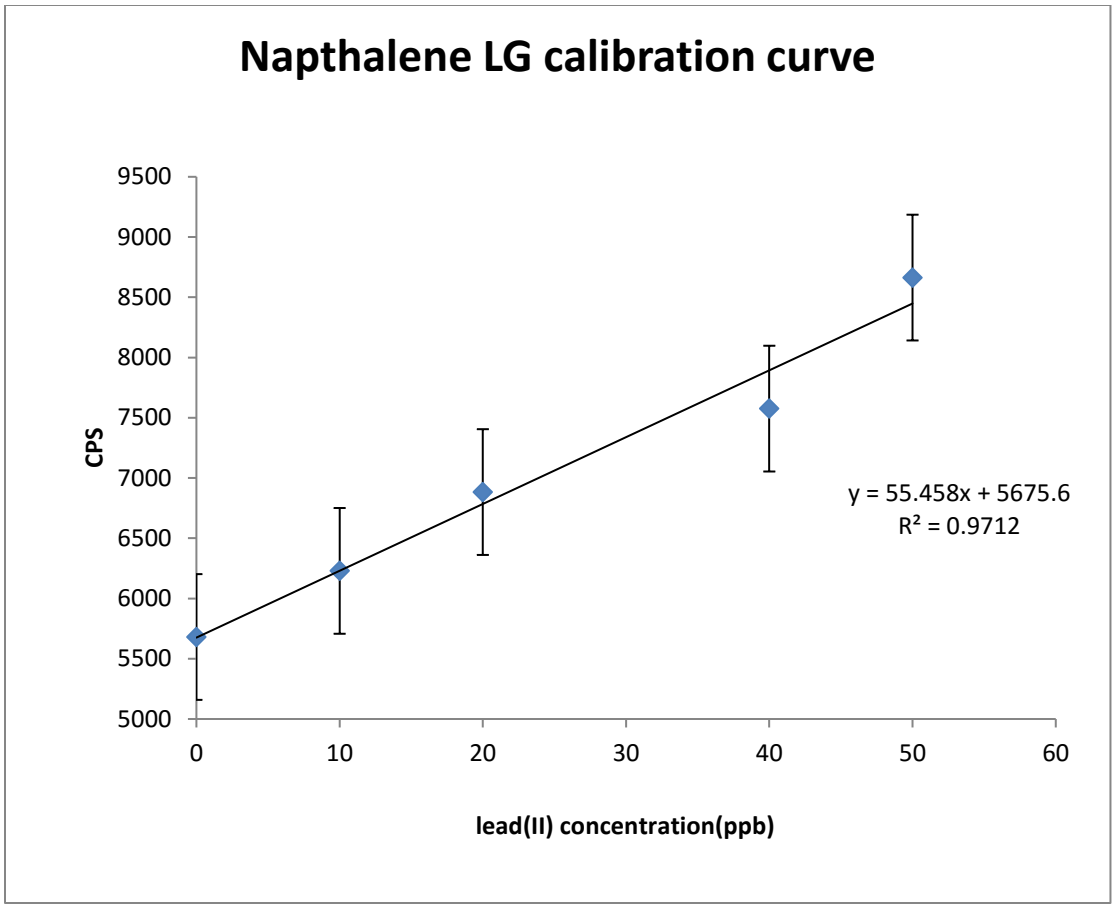

Figure 22: Napthalene LG dissolved in 50% acetone/water lead calibration curve using benchtop fluorometer maximum intensity. Excitation 389nm. Emission maximum: 527nm

The data shows a high background signal. This could be because there was still some un-hydrolyzed N-LG left in the sample. Since the binding protocol was optimized only for LG, there might have been limitations when dealing with N-LG. However, due to the larger Stokes shift for N-LG it may be worth looking into in the future.

Chapter 5: Water sample testing

5.1 Calibration data

Once the protocol had been optimized, the next step was to test water samples using LG. In order to do this a calibration curve was made using solutions of known concentration of lead between 0ppb and 50ppb mixed with the LG molecule and base. The calibration curve is shown in Figure 23.

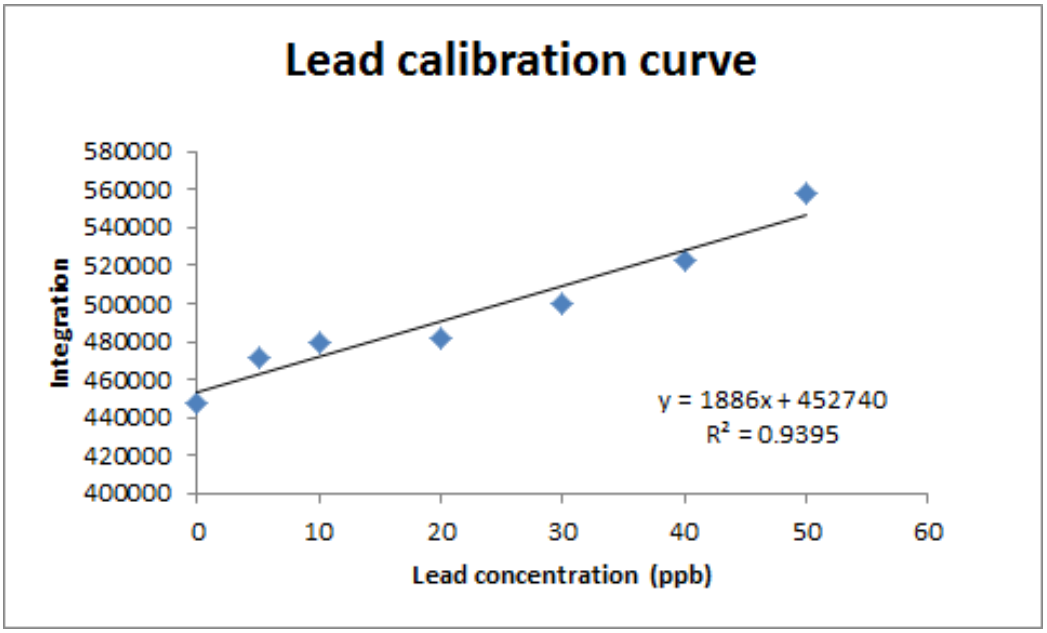

Figure 23: Lead calibration curve using LG on benchtop fluorometer taking total integration under emission curve. Excitation: 389nm, Emission: 410nm-550nm

Similar to the benchtop instrument, a calibration curve was established with known concentrations of lead for both prototype fluorometers, shown in Figure 24 and Figure 25.

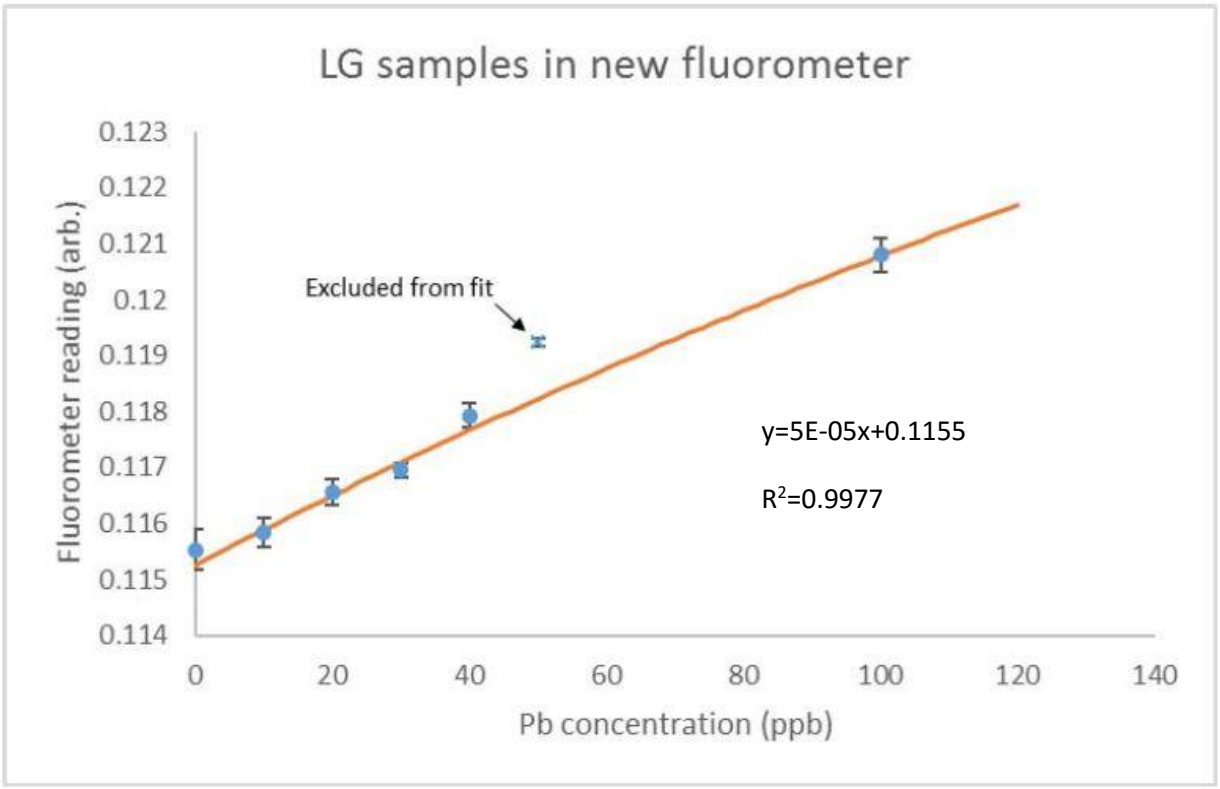

Figure 24: LG calibration curve using the second iteration prototype fluorometer. The line shown is approximate concentration using the Beer-Lambert law, while the equation is based on a linear fit to the data points.

The data point was excluded due to poor sample handling. The data shows a high background signal. This could be because there was still some un-hydrolyzed N-LG left in the sample. Since the binding protocol was optimized only for LG, there might have been limitations when dealing with N-LG. However, due to the larger Stokes shift for N-LG it may be worth looking into in the future.

5.2 Water sample testing using LG

Once the calibration curve was established samples from residences in an urban neighborhood in Pittsburgh were collected, with the permission of the residents as well as Internal Review Board (IRB) approval from Duquesne University. The IRB process involved going through the CITI training program in order to handle residents' water samples and information. A key was developed by the principal investigator, Dr. Partha Basu, for each house and kept in his office. Two samples were collected from each house, with a total of 18 samples from 9 houses. The residents signed a consent form and were instructed to collect a morning sample before they used water for the day, as well as an afternoon sample after they had been using the water as per normal household activities. Once the samples were collected they were stored in a refrigerated, 4 °C room until use. The samples were tested and the values were calculated from the calibration curve. Two different analysis methods were used to determine the lead content in the samples. The first, shown in Table 3 takes the integration of the emission spectrum between 410nm and 550nm, similar to how the portable fluorometer works. The second, shown in Table 4, takes the peak emission intensity and correlates it to a lead concentration based on the calibration curve.

Afternoon Sample	Calculated lead concentration (ppb)	Morning Sample	Calculated lead concentration (ppb)
1A	81.7	**1M**	16.9
2A	112.5	**2M**	10.4
3A	0	**3M**	47
5A	47	**5M**	39.1
6A	41.1	**6M**	42.7
7A	44.4	**7M**	44.1
8A	174.2	**8M**	30.2
9A	170	**9M**	41.6
11A	37.7	**11M**	52.8

A=Afternoon M=Morning

Table 3: Pittsburgh neighborhood water samples lead concentrations using integration method

Taking the integration of the data across the entire range yielded the data shown above in Table 3. This method reduces the impact of noise fluctuations across the entire spectrum, however, since the range is between 410nm and 550nm, there is a larger overlap from the excitation spectrum present. This would cause the lead values to be inflated. This can particularly be seen in the commercially available device, as the

readings from the device were consistently higher for the known concentrations of lead solution, which then started to saturate around 100ppb.

According to the data, the majority of the houses showed no difference in lead levels in the morning as compared to the afternoon. These results are not what were expected since the water collected in the morning would be stagnant, leaching more lead into the water.

Afternoon Sample	Calculated lead concentration (ppb)	Morning Sample	Calculated lead concentration (ppb)
1A	7.28	**1M**	39.11
2A	10.38	**2M**	20.1
3A	27.8	**3M**	21.1
5A	0	**5M**	0
6A	17.59	**6M**	62.54
7A	0	**7M**	11.79
8A	11.39	**8M**	9.28
9A	4.28	**9M**	7.18
11A	13.69	**11M**	16.79

Table 4: Pittsburgh neighborhood residents' water sample lead content using highest intensity

Taking the highest intensity of the emission spectrum at yielded the data shown above in Table 4. This method reduces the overlap emission from the excitation spectrum as the highest emission intensity is roughly at 427nm. However, after the resident's water samples were tested on the benchtop spectrofluorometer, they were tested on both iterations of the portable fluorometer for comparison. Similar to the benchtop

instrument, a calibration curve was established with known concentrations of lead for both prototype fluorometers, shown in Figure 26 and Figure 27.

Once the calibration curve was established, the residents' water samples were tested using the protocol mentioned. The results were initially recorded as an arbitrary voltage reading then converted to a corresponding lead concentration based on the calibration curve. The results are shown in Figure 26. The blue bar indicates a morning sample while the orange bar indicates an afternoon sample.

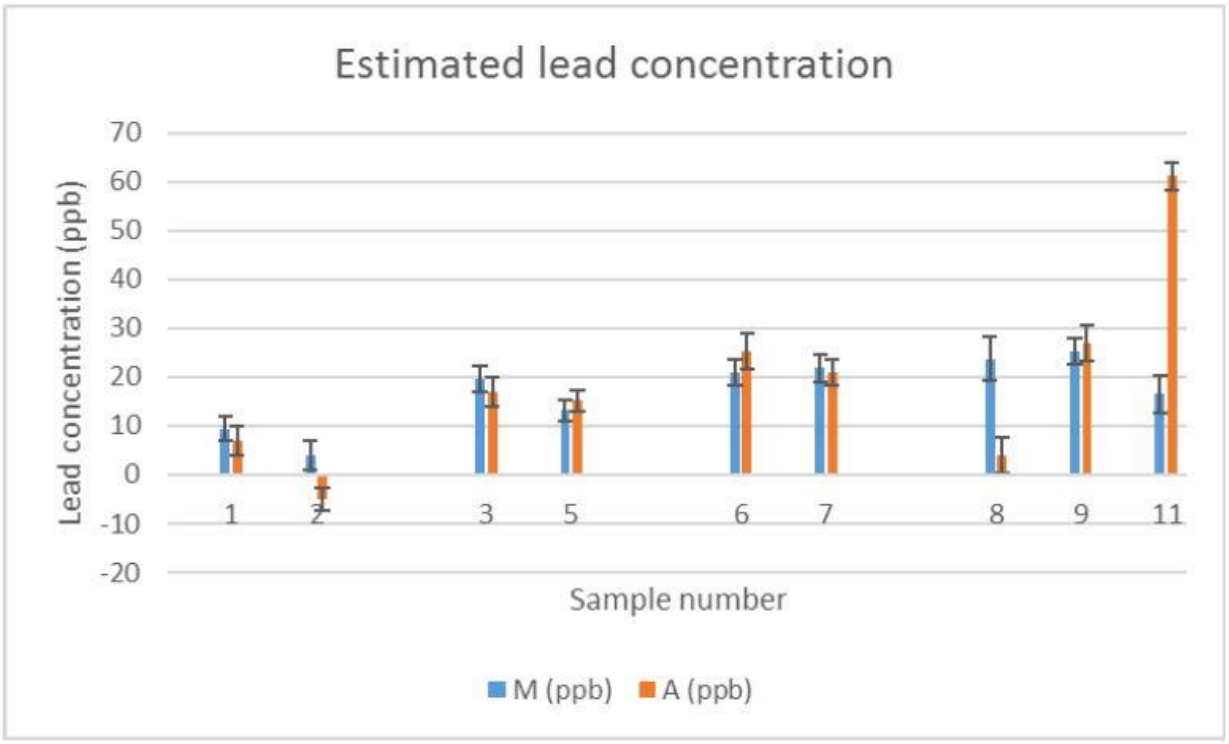

Figure 25: Residents' water samples with lead concentrations using portable fluorometer. Excitation: 390nm

The portable fluorometer and benchtop fluorometer data was compared against ICPMS. The ICPMS data is shown in Table 5.

Afternoon Sample	Calculated lead concentration (ppb)	Morning Sample	Calculated lead concentration (ppb)
	MCL		15ppb
1A	2.2	1M	0.3
2A	0.1	2M	0.3
3A	1.1	3M	0.3
5A	7.7	5M	7.4
6A	4.0	6M	3.8
7A	0.5	7M	0.5
8A	19.2	8M	1.6
9A	0.3	9M	6.3
11A	1.3	11M	1.6
13A	4.9	13M	6.6

Table 5: ICPMS data for water samples

According to the data, the portable fluorometer and bench top fluorometer greatly differed. The portable fluorometer showed no statistical difference between the morning and afternoon samples. This could be because the handling and sample preparation when testing on the portable fluorometer were not adequate. The samples

were not fixed with nitric acid, due to the low pH degrading the compound, therefore the Pb^{2+} content could have changed over time.

The benchtop instrument showed a higher lead concentration for the afternoon samples for a majority of the samples, which is not what was expected.

The ICPMS data showed that only one sample, **8A,** was above the Maximum Contaminant Level (MCL) for lead. The other data sets showed elevated lead levels for almost every sample. One possibility for this is that there are other interferences in the samples which either synergistically or individually increase the fluorescence signal. The calibration curves were done using ultrapure water, which would not have metal ions or other compounds which would increase the fluorescent signal, and therefore showed a linear increase with addition of lead.

Another possibility could be that the proximity of the excitation spectrum to the emission spectrum was causing some overlap to occur. This would cause the detector to read excess signal, causing a higher lead value than what is present in the sample.

When obtaining the data for the benchtop and portable fluorometers, two different techniques were used. The portable fluorometer takes the integration under the curve of the fluorescence emission based on the light entering the detector after the high-pass optical filter. In contrast, the benchtop fluorometer shows the entire fluorescence emission spectrum. The emission intensity is integrated between 415nm

and 515nm and correlated to a lead concentration based on the calibration curve. However, with an update to the software, integration of the benchtop spectrum was possible and was done over the total emission range of 410nm to 550nm for a more consistent set. Using the integration method on the benchtop fluorometer, the lead values were much higher than the ICPMS data.

Since the concentrations of lead are relatively low, sensitivity is an important factor when measuring the values. A benchtop instrument could be more suitable to measure lead concentration, as it is fitted with a xenon lamp for a high light intensity and an excitation and emission monochromator to admit specific wavelengths of light to both the sample chamber and detector respectively. However, the background signal is still high.

Incorporating such features into a portable device would not be practical, as the electricity needed to power the device would quickly drain the battery and price of the components would be too high. The current commercially available devices cost over $2,000 and do not have excitation wavelengths optimal for testing for Pb^{2+} with LG.

Chapter 6: Conclusion

A procedure was optimized for the binding of Pb^{2+} to the LG molecule and a protocol was established for testing water samples. The naphthalene LG derivative was also successfully synthesized and its lead binding properties as well as quantum yield were determined. The portable fluorometer will need to be further optimized to reduce background noise in order to quantify lead below the EPA action limit. In addition, the handling and transportation of samples as needs to be further optimized to ensure no differences between data sets.

The background on the portable fluorometer could be due to interference from the excitation spectrum or light entering or escaping the filter cube. In addition, adjusting the protocol to hydrolyze more LG could also reduce background signal. A step needs to be included to possibly remove other interfering compounds or metals from water samples. This step would ideally keep all Pb^{2+} in solution while removing other compounds. This can be done by either precipitating out other metals or by destroying the organic compounds in the samples.

The biggest issue with the experiment was that the lead concentration was inflated when analyzing water samples. As was evident in the commercially available device, the lead concentrations that the machine output were higher than the actual concentrations of the prepared solutions. This was also confirmed with the in-house

built fluorometer and benchtop fluorometer, which each showed a higher lead concentration than was actually present in the water samples. Both the integration method and highest intensity method showed inflated values for lead, with the integration being the highest.

In addition, testing 9 residences in a single neighborhood is too small a sample size to draw an adequate conclusion about whether there is an issue with lead. Additional testing will be need to be conducted in a variety of neighborhoods in Pittsburgh to get a broader picture of where high lead levels are located.

The Napthalene LG showed more promising fluorescence properties when compared to the original LG molecule. Its higher quantum yield means that more light is emitted from the fluorophore, which means that there will be a higher signal to noise ratio and therefore a better resolution can be achieved. In addition, a larger Stokes shift means there is less overlap between the excitation and emission spectra. This will make it easier to filter out the excitation light and therefore reduce background noise. Finally, the photodiodes being used are more responsive towards longer wavelengths of light, which will increase the signal going to the detector. A lower background coupled with a higher signal going to the detector will mean that a lower Pb^{2+} concentration can be detected. However, issues with its solubility make it a difficult

compound to use in a field setting. Additional functional groups need to be added to the molecule to make the solubility more suitable for a field setting.

At nearly a fraction of the cost, the portable fluorometer is a feasible method to quantify Pb^{2+} in water, with additional changes to sample preparation and handling. In addition, the portable method cuts down on costs and time of transporting samples to a lab and potential cross-contamination of the samples with other sources of Pb^{2+}. As Flint, Michigan showed, citizens are willing and able to test their own water for lead given the means to do so.

References

1. "Air Quality Criteria for Lead (2006) Final Report" (EPA/600/R-05/144aF-bF). Washington, DC: U.S. Environmental Protection Agency, 2006. http://cfpub.epa.gov/ncea/cfm/recordisplay.cfm?deid=158823#Download. Accessed July 2016.
2. Abadin, H., Ashizawa, A., Stevens, Y.W., et al. *Toxicological Profile for Lead*. Atlanta, GA: Agency for Toxic Substances and Disease Registry (US), 2007.
3. Apostoli, P., et. al. *Elemental Speciation in Human Health Risk Assessment*. World Health Organization, 2006.
4. CDC Advisory Committee on Childhood Lead Poisoning Prevention. "Low level lead exposure harms children: a renewed call for primary prevention." Atlanta, GA: US Department of Health and Human Services, CDC, 2012. http://www.cdc.gov/nceh/lead/acclpp/final_document_030712.pdf.
5. Rhoads, G. G. "Low Level Lead Exposure Harms Children." Advisory Committee on Childhood Lead Poisoning of the Centers for Disease Control and Prevention. January 2012.
6. Centers for Disease Control. "Blood Lead Levels in Children." http://www.cdc.gov/nceh/lead/ACCLPP/Lead_Levels_in_Children_Fact_Sheet.pdf . Accessed August 2016.
7. "Integrated Science Assessment for Lead (Third External Review Draft)" (EPA/600/R-10/075C). Washington, DC: U.S. Environmental Protection Agency, 2012.
8. Etzel, R. A., Balk, S. J., eds. *Pediatric Environmental Health*. 2nd ed. Elk Grove Village, IL: American Academy of Pediatrics, 2003
9. Florea, A., Taban, J., Varghese, E., Alost, B. T., Moreno, S., and Büsselberg, D. "Lead (Pb2+) neurotoxicity: Ion-mimicry with calcium (Ca2+) impairs synaptic transmission" (A review with animated illustrations of the pre- and post-synaptic effects of lead). *Journal of Local and Global Health Science* 4 (2013). http://dx.doi.org/10.5339/jlghs.2013.4
10. U.S Consumer Protection Safety Commission. "CPSC Announces Final Ban on Lead-Containing Paint." September 7th, 1977. https://www.cpsc.gov/en/Recalls/1977/CPSC-Announces-Final-Ban-On-Lead-Containing-Paint/. Accessed September 2016.
11. Evens, A., et al. "The Impact of Low-Level Lead Toxicity on School Performance among Children in the Chicago Public Schools: A Population-Based Retrospective Cohort Study." *Environmental Health* 14 (2015): 21. PMC. Web. 26 May 2016.

12. "National Ambient Air Quality Standards for Lead" Final Rule. Environmental Protection Agency. 73 FR 66963. November 12, 2008.
13. "The Lead Disclosure Rule." US Department of Housing and Urban Development. 24 CFR Part 35. http://portal.hud.gov/hudportal/documents/huddoc?id=DOC_12347.pdf. Accessed September 2016.
14. Tiemann, M. "Safe Drinking Water Act (SDWA): A Summary of the Act and Its Major Requirements." Congressional Research Service. February 5, 2014.
15. "Prohibition on use of lead pipes, solder, and flux." Safe Drinking Water Act Amendments of 1986. 42 U.S.C. § 300g-6(d). Pub.L. 99–359. June 19, 1986.
16. "Maximum Contaminant Level Goals and National Primary Drinking Water Regulations for Lead and Copper" Final Rule. Environmental Protection Agency. 56 FR 26460. 40 CFR Part 141, Subpart I. June 7, 1991.
17. "Lead and Copper Rule: A Revised Quick Reference Guide" (EPA 816-F-08-018). Washington, DC: U.S. Environmental Protection Agency, 2008. http://nepis.epa.gov/Exe/ZyPDF.cgi?Dockey=60001N8P.txt
18. Edwards, M., et. al. "Lead testing results for water sampled by residents." http://flintwaterstudy.org/information-for-flint-residents/results-for-citizen-testing-for-lead-300-kits/. Accessed August 2016.
19. "The Analysis of Drinking Waters by U.S. EPA Method 200.8 using the NexION 300Q ICP-MS in Standard Mode." Application Note. PerkinElmer Inc., 2012.
20. Fan, F., et. al. "Determination of Lead by Square Wave Anodic Stripping Voltammetry Using an Electrochemical Sensor." *Analytical Sciences*. 29 (2013).
21. Marbella, L., Serli-Mitasev, B., and Basu, P. "Development of a Fluoresecent Pb^{2+} sensor." *Angew. Chem. Int. Ed.* 48, 3996-3998 (2009).
22. The University of Texas at Austin. "ICP-MS?" Jackson School of Geosciences, 2016. http://www.jsg.utexas.edu/icp-ms/icp-ms/.
23. Abadin, H., Ashizawa, A., Stevens, Y. W., et al. "Analytical Methods." *Toxicological Profile for Lead*. Atlanta, GA: Agency for Toxic Substances and Disease Registry (US), 2007. http://www.ncbi.nlm.nih.gov/books/NBK158761/.
24. Zinterhofer, L. J. M., Jatlow, P. I. and Fappiano, A. "Atomic Absorption Determination of Lead in Blood and Urine in the Presence of EDTA." *J. Lab. Clin. Med.* 78, 664 (1971).
25. IUPAC. "Beer–Lambert law." *Compendium of Chemical Terminology*. Online corrected version. 2006.
26. "Lead Ban: Preventing the Use of Lead in Public Water Systems and Plumbing Used for Drinking Water" (570/9-89-BBB). United States Environmental Protection Agency, 1989.

27. Highly Sensitive Electrochemical Determination of Lead in Tap Water. Copyright © 2013 Pine Research Instrumentation DRL10008 REV001 (SEP 2013)
28. "Application Note S-6: Fundamentals of Stripping Voltammetry." Princeton Applied Research.
29. Harvey, D., and Valeur, B. *Modern Analytical Chemistry. Molecular Fluorescence: Principles and Applications.* Germany: Wiley 2001.
30. Meng, X., Wang, S., and Zhu, M. *Quinoline-Based Fluorescence Sensors, Molecular Photochemistry*. InTech, 2012.
31. Demchenko, A. P. *Introduction to Fluorescence Sensing*. 2nd edition. Switzerland: Springer International Publishing, 2015.
32. Ceroni, P. *The Exploration of Supramolecular Systems and Nanostructures by Photochemical Techniques*. 14th edition. Netherlands: Springer, 2012.
33. Wang, Y., Yang, M-Y., Zheng, M-H., Zhao, X-L., Xie, Y-Z., Jin, J-Y. "2-Pyridylthiazole derivative as ICT-based ratiometric fluorescent sensor for Fe(III)." *Tetrahedron Letters* 57.22, 2399-2402 (2016).
34. Xuan, W., et. al. "Reaction-Based 'Off–On' Fluorescent Probe Enabling Detection of Endogenous Labile Fe^{2+} and Imaging of Zn^{2+}-induced Fe^{2+} Flux in Living Cells and Elevated Fe^{2+} in Ischemic Stroke." *Bioconjugate Chem* 27.2, 302–308 (2016).
35. Wozniak, A. K., et. al. "Single-molecule FRET measures bends and kinks in DNA." *PNAS* 105.47, 18337-18342 (2008).
36. Kwon, J. Y., et. al. "A highly Selective Fluorescent Chemosensor for Pb^{2+}." *J. AM. Chem. Soc.* 127.128 (2005).
37. Housecroft, C. E. and Sharpe, A. *Inorganic Chemistry*. 2nd edition. England: Pearson Education Ltd., 2005.
38. Horiba Scientific. Fluoromax 4 Operation Manual: Part number 810005 version B. Edison, NJ: 2009.
39. Paschotta. R. "Dichroic mirrors." *Encyclopedia of Laser Physics and Technology.* Wiley, 2008.
40. Wei, L**.,** Fujiwara, K., and Fuwa, K. *Anal. Chem* 55, 951-955 (1983)**.**
41. Abadin, H., Ashizawa, A., Stevens, Y. W., et al. *Toxicological Profile for Lead*. Atlanta, GA: Agency for Toxic Substances and Disease Registry (US), 2007.
42. Olmsted, J. and Williams, G. *CRC Handbook of Chemistry and Physics, Chemistry*. 5th edition. Wiley, 2004.
43. Huffman Hazen Laboratories. "ICP-MS Analysis" http://www.huffmanlabs.com/?page_id=122. Accessed October 2016.
44. Gibbs, C. R. *Simplified Testing for Lead and Copper in Drinking Water*. Technical Information Series—Booklet No. 19. Hach Company, 1994.

45. Spear, J. M., et. al. "Evalution of arsenic field test kits for drinking water analysis." *Journal AWWA* 98.12 (2006).
46. Cai-Ling, F., et. al. "A Quinoline Derivated Chemosensor for Cu^{2+} Recognition." *Chem. Res. Chinese Universities* 25.5, 620-623 (2009).
47. Diebler, K. The Development of a New Generation of Fluorescent Sensors. Duquesne University, Pittsburgh, PA. May 2012.

Appendix

Duquesne University IRB
Protocol #2016-05-9
Approved: 5-27-2016
Expiration Date: 5-26-2017

DUQUESNE UNIVERSITY

600 FORBES AVENUE ♦ PITTSBURGH, PA 15282

CONSENT TO PARTICIPATE IN A RESEARCH STUDY

TITLE:	Detection of Lead in Waters in the Homes of Local Residents
INVESTIGATOR:	Aria Parangi, Bayer School of Natural and Environmental Science, parangia@duq.edu, [redacted]
ADVISOR:	Partha Basu, Bayer School of Natural and Environmental Science, basu@duq.edu, 412.396.6345
SOURCE OF SUPPORT:	This study is being performed as partial fulfillment of the requirements for the Masters degree in the Environmental Science and Management program at Duquesne University.
PURPOSE:	You are being asked to participate in a research project that seeks to determine the lead concentration in household waters.
PARTICIPANT PROCEDURES	To participate in this study, you will be asked to: collect water samples from a faucet in your home. We will give you two tubes to collect samples: in the tube marked as morning, you will collect pre-flush water and in the tube marked as evening, you can collect samples anytime after noon, as long as the faucet is being used. We will collect the water samples, taken them to Duquesne University, and analyze for lead. If you are interested in knowing the results, please let us know, and we will mail you the results. For that we will also collect your address. Only the investigator will know which resident has how much lead in their water.
RISKS AND BENEFITS:	There are minimal risks associated with this participation but no greater than those encountered in everyday life. By participating in this study you will be benefitting the local community and the research at large.
COMPENSATION:	There will be no compensation for participation in this study. Participation in the project will require no monetary cost to you.

Duquesne University IRB
Protocol #2016-05-9
Approved: 5-27-2016
Expiration Date: 5-26-2017

CONFIDENTIALITY: Your participation in this study and any personal information that you provide will be kept confidential at all times and to every extent possible.

Your name will never appear on any survey or research instruments. All written and electronic forms and study materials will be kept secure. Any study materials with personal identifying information will be maintained for three years after the completion of the research and then destroyed.

RIGHT TO WITHDRAW: You are under no obligation to participate in this study. You are free to withdraw your consent prior to sample collection. After that all identifiers will be removed from the samples and the information can be used for statistical purposes only.

SUMMARY OF RESULTS: A summary of the results will be mailed to you, at no cost, upon request.

VOLUNTARY CONSENT: I have read the above statements and understand what is being requested of me. I also understand that my participation is voluntary and that I am free to withdraw my consent at any time, for any reason. On these terms, I certify that I am willing to participate in this research project.

I understand that should I have any further questions about my participation in this study, I may call Aria Parangi at [redacted] or Partha Basu at 412-396-6345. Should I have questions regarding protection of human subject issues, I may call Dr. Linda Goodfellow, Chair of the Duquesne University Institutional Review Board, at 412.396.1886.

_____ _____

Participant's Signature Date

_____ _____

Researcher's Signature Date